OPTIMIZATION OF POWER SPECTRA OF MULTIWAVEGUIDE GRILLS

Horst D. Pacher

IPP 2/247 December 1979

MAX-PLANCK-INSTITUT FÜR PLASMAPHYSIK

8046 GARCHING BEI MÜNCHEN

MAX-PLANCK-INSTITUT FÜR PLASMAPHYSIK

GARCHING BEI MÜNCHEN

OPTIMIZATION OF POWER SPECTRA OF MULTIWAVEGUIDE GRILLS

Horst D. Pacher

IPP 2/247 December 1979

Die nachstehende Arbeit wurde im Rahmen des Vertrages zwischen dem Max-Planck-Institut für Plasmaphysik und der Europäischen Atomgemeinschaft über die Zusammenarbeit auf dem Gebiete der Plasmaphysik durchgeführt.

IPP 2/247 H.D. PACHER

Optimization of Power Spectra of Multiwaveguide Grills

(in English)

December 1979

ABSTRACT : To optimize the power spectrum of multielement grill structures, a simplified formulation of the grill coupling theory is developed. The optimization criteria are identified as : high ratio of accessible to inaccessible power, low ratio of nominal power to actual power when electric field limitations exist and flexibility in the principal parallel wavenumber coupled to the plasma while preserving the first two criteria. General conditions on the configuration are deduced, and applied to the present WEGA grill and future multielement grills (12-16 waveguides) for WEGA and larger experiments. A novel grill arrangement, the " even " grill, is proposed and found to give excellent results.

I. INTRODUCTION

Lower hybrid heating is an attractive candidate for additional heating of Tokamaks. Its attractiveness is enhanced by the availability of tubes in the GHz range and by the simplicity of the coupling structure consisting of a phased array of waveguides, the "grill", first proposed in 1) and extensively treated theoretically by a number of authors (2-8) . Present experimental results have indicated good heating (eg 11) However, to the date of writing, no high-power heating experiments have been performed for which the exciting structure is longer than 1/2 period of the principal (slow) peak of the parallel wavelength spectrum. As a result, in these experiments a large part of the applied power, typically 30-50%, is excited at wavenumbers too low to fulfil the accessibility condition (9) and therefore is not expected to penetrate to the plasma center. With this proviso, the efficiency of heating has been reasonable - for example, in the WEGA experiment (11), about 40% of the applied HF power was transferred to the plasma ions and electrons (in the ratio of about 1 : 2). However, these experiments were accompanied by unwanted effects, such as an increase of the plasma density . To increase overall efficiency and reduce the unwanted effects, the inaccessible fraction of the power must be reduced. The optimization of the power spectrum to maximize the accessible power is one of the main purposes of this report.

Nevertheless, the quality of the transmitted spectrum of parallel wavenumber is not the only criterium governing the applicability of the grill. A second very important criterium is the possibility of dynamic tailoring of the spectrum in order to maintain optimal heating as the plasma parameters, and therefore the desired wavenumbers, change in the course of the heating. Practically, this may be accomplished by either grouping the waveguides in discrete groups having the same phase (relative phases 0 or π, i.e. standing wave), or by progressively dephasing the waveguides by an angle ϕ, different from 0 or π, which is variable in time (travelling wave case). The spectrum resulting from various standing-wave groupings and from the travelling-wave case will be discussed in detail.

Finally, a third criterium of grill quality is the power transferrable by the grill if each waveguide is limited in the local electric field permissible due to breakdown or multipactor effect. The grill as a whole is never perfectly matched to the plasma. Indeed, a plasma possessing either very low or very high density gradients in front of a grill will reflect almost all the power. We shall define a quality factor Q, the ratio of nominal power transferred in the absence of reflection and at equal power density in the entire grill, to actual power transferred in the presence of the plasma under the best plasma conditions in the worst waveguide of the grill. This factor should be as small as possible. In order to achieve this, all the waveguides of the grill must have minimum reflection at roughly the same density gradient, which will necessitate an amplitude modulation of incident power in the grill.

In order to permit the synthesis of grills satisfying the above criteria, a simplified form of the grill coupling theory of Brambilla (Ref. 2,8) is deduced. The expressions for the power spectrum, the grill reflection coefficients, and the quality factor Q are deduced. The structure of the power spectrum is examined in detail for various standing-and travelling-wave configurations, and conditions for good definition of the spectrum are deduced. These conditions are then applied to a series of simplified grills with infinitely thin walls, and, finally, to a series of realistic grills.

II. MATCHING OF WAVEGUIDES TO PLASMA

In the following theoretical section, we follows closely the approximations of Krapchev and Bers (Ref. 7). The major approximation made in their paper is the neglect of the higher order evanescent modes. For a full treatment of the problem including these modes, the reader is referred to the paper by Brambilla (Ref. 8), in which the problem is treated fully. In order to obtain tractable equations which permit optimization of the multi-waveguide problem in the presence of reflections, we also neglect the higher order modes.

We shall use a slab model, in which x is the direction of the density gradient, z is the direction along the magnetic field. We shall assume the waveguide to be infinitely high in the y-direction. Consequently, we set all derivatives with respect to y to zero ($\frac{\partial}{\partial y} \equiv 0$). All dimensions are normalized to the free-space wavenumber ($x \equiv \frac{\omega}{c}$ x space $\equiv 2\pi \frac{\text{x space}}{\lambda_0}$). The fields in the k^{th} of the ℓ wave-guides composing the grill may be written, if one writes $E_z(x, z, t) = \mathcal{R}e\, E_z(x, z)\, e^{-i\omega t}$

$$E_z^k(x,z) = \left(E_{ik} e^{ix} + E_{rk} e^{-ix}\right) g_k(z) \tag{1a}$$

$$H_y^k(x,z) = -Y_0 \left(E_{ik} e^{ix} - E_{rk} e^{-ix}\right) g_k(z) \tag{1b}$$

where Y_0 is the wave admittance of the fundamental TM_0 mode in the guide, and is equal, for our case of infinitely high waveguides, to the inverse of the free-space impedance ($Z_0 = \sqrt{\mu_0/\varepsilon_0}$). The function $g_k(z)$ is the space function of the k^{th} guide and is defined as

$$\begin{aligned} g_k(z) &= u(z_k - b_k/2) - u(z_k + b_k/2) \\ &= 1 \qquad z_k - b_k/2 \le z \le z_k + b_k/2 \\ &= 0 \qquad \text{elsewhere} \end{aligned} \tag{2}$$

and where the k^{th} waveguides has a width along z of b_k and is centered at $z = z_k$. x is measured from the waveguide mouth toward the plasma.

We note in passing the relationship between the modes (TM_m and TE_m)of the infinitely high waveguide and the more familiar modes of the rectangular waveguide. The identification of the modes may be carried out by writing the fields of the modes of the rectangular waveguide around half-height, letting the total height go to infinity, and comparing with the fields of the modes of the infinitely high guide. Hence the TM_0 mode of the infinite waveguide (which is actually TEM), the fundamental mode, is found to be equivalent to the TE_{10} mode and has wave impedance and propagation constant equal to the free-space case. The TM_m modes are found to be equivalent to the TM_{1m} modes of the rectangular guide for $m \neq 0$ (m=0 does not exist in the rectangular guide), and the TE_m modes to the rectangular TE_{om} modes. The amplitude of the TE_{1m} modes and all modes with a first index greater than 1 go to zero as we let the height go to infinity.

In the plasma region, we write E_z and H_y in terms of their Fourier transforms :

$$E_z^{pl}(x,z) \equiv \frac{1}{\sqrt{2\pi}} \int_{-\infty}^{\infty} dn_z \; \mathcal{E}_z(x,n_z) e^{in_z z} \qquad 3a)$$

$$H_y^{pl}(x,z) \equiv \frac{1}{\sqrt{2\pi}} \int_{-\infty}^{\infty} dn_z \; \mathcal{H}_y(x,n_z) e^{in_z z} \qquad 3b)$$

To match the electric fields in the plasma ($x=0^+$) to the fields as the waveguide mouth ($x = 0^-$) , que require continuity of the electric field across the entire surface x = 0.
Hence we equate 1a) and 3a) to obtain, after Fourier transformation

$$\mathcal{E}_z(0^+, n_z) = \sum_{m=1}^{\ell} (E_{im} + E_{rm}) \, G_m(n_z) \qquad (4)$$

where $G_m(n_z)$ is the Fourier transform of the space function $g_m(z)$ of the m'th waveguide, i.e.

$$G_m(n_z) = \frac{1}{\sqrt{2\pi}} \int_{-\infty}^{\infty} dz \; g_m(z) e^{-in_z z} = \sqrt{\frac{2}{\pi}} \; \frac{e^{-in_z z_m} \sin \frac{n_z b_m}{2}}{n_z} \qquad (5)$$

The magnetic fields may not be so easily matched because of the presence of surface currents in the walls, which also depend on the higher order evanescent modes not considered here. We shall assume that the <u>average</u> magnetic field of the fundamental across the waveguide mouth equals the average of the plasma magnetic field. That is, we assume that the contribution of the evanescent modes to the average magnetic field at each waveguide mouth is negligible. While this assumption seems reasonable, it can only be justified by comparison of the results of the simplified model with those of the complete model (Ref. 8).

Accordingly, we set equal the integrals of 1b) and 3b) across each waveguide mouth to obtain the ℓ equations.

$$E_{ik} - E_{rk} = \frac{1}{Y_0 b_k} \int_{-\infty}^{\infty} dn_z \; Y_{pl}(n_z) \mathcal{E}_z(0, n_z) G_k^*(n_z) \qquad (6)$$

$$k = 1 \ldots \ell$$

where we have indentified, using 5)

$$\frac{1}{\sqrt{2\pi}} \int_{z_k - b_k/2}^{z_k + b_k/2} dz \, e^{in_z z} = G_k^*(n_z)$$

In the above, we have introduced the surface admittance of the plasma.

$$Y_{pl}(n_z) \equiv -\frac{\mathcal{H}_y(0,n_z)}{\mathcal{E}_z(0,n_z)} \tag{7}$$

defined by analogy with the wave admittance, but using the Fourier transforms of the total field rather than incident and reflected fields separately. This quantity is calculated in the next section.

III- FIELDS IN THE PLASMA ; SURFACE ADMITTANCE OF PLASMA

The electric field in the plasma is the solution of

$$\nabla\times(\nabla\times\underline{E}) - \frac{\omega^2}{c^2}\underline{\underline{K}}\cdot\underline{E} = 0 \tag{8}$$

where $\underline{\underline{K}}$ is the dielectric tensor, normalized to ε_0, for a cold, two-fluid plasma given by Stix (Ref. 10). The magnetic fields are deduced from

$$\nabla\times\underline{H} = \varepsilon\frac{\partial}{\partial t}(\underline{\underline{K}}\cdot\underline{E}) \tag{9}$$

Four our case, $\frac{\partial}{\partial y} = 0$, (infinite height waveguides, slab model).
We rescale the space variables ($x = \frac{\omega}{c}x_{space}$)Fourier transform in the z direction, and substitute the components of $\underline{\underline{K}}$ to obtain

$$\frac{\partial^2}{\partial x^2}\mathcal{E}_z(x,n_z) + (n_z^2 - S)\left(-\frac{P}{S}\right)\mathcal{E}_z(x,n_z) + \frac{n_z D}{S}\frac{\partial}{\partial x}\mathcal{E}_y(x,n_z) = 0 \tag{10}$$

$$\frac{\partial^2}{\partial x^2}\mathcal{E}_y(x,n_z) + \left(\frac{D^2}{n_z^2-S} - (n_z^2-S)\right)\mathcal{E}_y(x,n_z) + \frac{n_z D}{n_z^2-S}\frac{\partial}{\partial x}\mathcal{E}_z(x,n_z) = 0 \tag{11}$$

$$\mathcal{E}_z(x,n_z) = -\frac{i}{n_z^2-S}\left(n_z\frac{\partial}{\partial x}\mathcal{E}_z(x,n_z) + D\mathcal{E}_y(x,n_z)\right) \tag{12}$$

$$\mathcal{H}_y(x,n_z) = \frac{1}{n_z z_0}\left(S\mathcal{E}_x(x,n_z) - iD\mathcal{E}_y(x,n_z)\right) \tag{13}$$

Where Z_0 is again the free-space impedance, and S, P, D are the notations introduced by Stix (Ref. 11).

From (12) and (13), we find

$$Y_{pe}(n_z) \equiv -\frac{\mathcal{H}_y(0,n_z)}{\mathcal{E}_z(0,n_z)} = \frac{iS}{Z_0(n_z^2-S)} \lim_{x\to 0}\left[\frac{1}{\mathcal{E}_z}\frac{\partial \mathcal{E}_z}{\partial x} + \frac{D}{S} n_z \frac{\mathcal{E}_y}{\mathcal{E}_z}\right] \quad (14)$$

We note that the Poynting vector corresponding to the plane wave n_z is given by

$$S_{pe,x} \equiv -\frac{1}{2}\,\mathrm{Re}\,(\mathcal{E}_z \mathcal{H}_y^*) = \frac{1}{2}|\mathcal{E}_z|^2\,\mathrm{Re}\,Y_{pe}(n_z) \quad (15)$$

In the lower hybrid frequency range, $\omega_{ci} << \omega << \omega_{ce}$, and therefore

$$S \approx 1 + \frac{\omega_{pe}^2}{\omega_{ce}^2} - \frac{\omega_{pi}^2}{\omega^2}\ ; \quad D \approx \frac{\omega_{pe}^2}{\omega\omega_{ce}}\ ; \quad P \approx 1 - \frac{\omega_{pe}^2}{\omega^2} \quad (16)$$

We shall assume, with Krapchev and Bers, that coupling to the fast wave may be neglected (i.e. last term of (10) is negligible, $|\varepsilon_y| << |\varepsilon_z|$ Furthermore, we assume that, at the waveguide mouth, the density corresponds to the slow-wave cutoff density ($\omega_{pe} = \omega$) or that the evanescence region of the slow wave is so small that perfect tunneling is achieved. Further, we assume that $S \simeq 1$, which is the case far from the resonance and in the edge plasma for $n_z > n_z$ acc. The reader is referred to the elegant summary by Brambilla (Ref. 8 , Sections 3 and 4) for a complete treatment of the validity of these approximations.
With the above approximations, we have

$$\frac{\partial^2}{\partial x^2}\mathcal{E}_z(x,n_z) + (n_z^2-1)\frac{\omega_{pe}^2}{\omega^2}\mathcal{E}_z(x,n_z) = 0 \quad (17)$$

and (19)

$$Y_{pe}(n_z) = \frac{i}{Z_0(n_z^2-1)} \lim_{x \to 0} \frac{1}{\mathcal{E}_z} \frac{\partial \mathcal{E}_z}{\partial x}$$

where (19) is particularly well justified because, at x = 0, $\frac{D}{S}$ is small ($\sim \omega/\omega_{ce}$ and $\varepsilon_y(0,n_z)$ is also small (since, for the fundamental, there is only an E_z field).

We shall now proceed to solve Equation (17) for the case of a linear density gradient on the plasma. We define

$$\alpha \equiv \frac{c}{\omega^3} \left(\frac{\omega_p^2}{n} \right) \cdot \nabla n \tag{20}$$

or, numerically

$$\alpha^{1/3} = \frac{15.67}{f_G} (\nabla n_{13})^{1/3} \tag{21}$$

Where f_G is the frequency in GHz and ∇n_{13} is the density gradient at the edge in units of 10^{13} cm^{-4}. Defining also

$$\zeta \equiv |n_z^2 - 1|^{2/3} \alpha^{1/3} x \tag{22}$$

(17) may be rewritten

$$\frac{\partial^2}{\partial \zeta^2} \mathcal{E}_z - \zeta \mathcal{E}_z = 0 \qquad |n_z| < 1 \tag{23}$$

$$\frac{\partial^2}{\partial \zeta^2} \mathcal{E}_z + \zeta \mathcal{E}_z = 0 \qquad |n_z| > 1 \tag{24}$$

a) Solution for $|n_z| < 1$

The solution is given by the Airy functions of positive argument. However, since Bi (ζ) diverges as ζ (i.e. x) goes to infinity, the complete solution is

$$\mathcal{E}_z(x, n_z) = C' \, Ai(\zeta) \qquad |n_z| < 1 \tag{25}$$

As $|\zeta|$ goes to zero,

$$\lim_{\zeta\to 0} Ai(\zeta) = \frac{1}{3^{2/3}\,\Gamma(2/3)} \;;\; \lim_{\zeta\to 0} \frac{d}{d\zeta} Ai(\zeta) = \frac{-1}{3^{1/3}\,\Gamma(1/3)}$$

Hence, using (19)

$$Y_{pl}(n_z) = \frac{e^{i\pi/2}\,\alpha^{1/3}}{Z_0\,|1-n_z^2|^{2/3}} \cdot \frac{3^{2/3}\,\Gamma(2/3)}{3^{1/3}\,\Gamma(1/3)} \qquad |n_z|<1 \tag{26}$$

We note that, since $Y_{p\ell}(n_z)$ is purely imaginary, the Poynting vector in the x direction given by (15) is zero, i.e. no power is transferred to the plasma for $|n_z| < 1$.

b) Solution for $|n_z| > 1$

For this case, the two linearly independent solutions of (24) are the Airy functions of negative argument $Ai(-\zeta)$ and $Bi(-\zeta)$. These are defined as

$$Ai(-\zeta) = \frac{1}{3}\sqrt{\zeta}\left[J_{-1/3}\left(\frac{2}{3}\zeta^{3/2}\right) + J_{+1/3}\left(\frac{2}{3}\zeta^{3/2}\right)\right]$$

$$Bi(-\zeta) = \frac{1}{\sqrt{3}}\sqrt{\zeta}\left[J_{-1/3}\left(\frac{2}{3}\zeta^{3/2}\right) - J_{+1/3}\left(\frac{2}{3}\zeta^{3/2}\right)\right] \tag{27}$$

$$Ai'(-\zeta) \equiv -\frac{d}{d\zeta}Ai(-\zeta) = \frac{1}{3}\zeta\left[-J_{-2/3}\left(\frac{2}{3}\zeta^{3/2}\right) + J_{+2/3}\left(\frac{2}{3}\zeta^{3/2}\right)\right]$$

$$Bi'(-\zeta) \equiv -\frac{d}{d\zeta}Bi(-\zeta) = \frac{1}{\sqrt{3}}\zeta\left[+J_{-2/3}\left(\frac{2}{3}\zeta^{3/2}\right) + J_{+2/3}\left(\frac{2}{3}\zeta^{3/2}\right)\right] \tag{28}$$

The Wronskian of the Airy Functions is given by

$$W(Ai, Bi) \equiv Ai\,Bi' - Bi\,Ai' = \frac{1}{\pi} \tag{29}$$

The field is given by a linear combination of Ai and Bi, i.e.

$$\mathcal{E}_z = C\,Ai(-\zeta) + D\,Bi(-\zeta) \tag{30}$$

Using (15), (13), (30), and(29), the Poynting vector may be simply written (in MKS units) as

$$S_{x,p\ell} \equiv -\frac{1}{2}\,\mathrm{Re}\left(\mathcal{E}_z \mathcal{H}_y^*\right) = \frac{\alpha^{1/3}}{2\pi Z_0\,|n_z^2-1|^{2/3}}\,\mathrm{Im}\,DC^* \tag{32}$$

We now apply the radiation condition at large ζ, i.e. we require that no energy be reflected from infinity. To implement this condition, we use the asymptotic expansion of the Airy Functions,

$$\lim_{\zeta \to \infty} Ai(-\zeta) = \frac{1}{\sqrt{\pi}\,\zeta^{1/4}} \cos\left(\tfrac{2}{3}\zeta^{3/2} - \pi/4\right)$$

$$\lim_{\zeta \to \infty} Bi(-\zeta) = \frac{-1}{\sqrt{\pi}\,\zeta^{1/4}} \sin\left(\tfrac{2}{3}\zeta^{3/2} - \pi/4\right) \qquad (33)$$

and calculate the square of the magnitude of the electric field

$$\lim_{\zeta \to \infty} \mathcal{E}_z \mathcal{E}_z^* = \frac{1}{2\pi \zeta^{1/2}} \Big[|C|^2 + |D|^2 + \left(|C|^2 - |D|^2\right) \cos 2\left(\tfrac{2}{3}\zeta^{3/2} - \pi/4\right) - \mathrm{Re}\, DC^* \sin 2\left(\tfrac{2}{3}\zeta^{3/2} - \tfrac{\pi}{4}\right) \Big] \qquad (34)$$

For a pure incident (or pure reflected) wave, the standing wave ratio must be 1 i.e. the magnitude of the electric field must be slowly varying with ζ while the phase varies rapidly. Hence we deduce from (34)

$$|C| = |D| \;; \quad \mathrm{Re}\, DC^* = 0 \qquad (35)$$

which implies

$$\frac{D}{C} = \pm i \qquad (36)$$

Since, for a pure incident wave, the Poynting vector is positive, we see from (32) that we must choose the + sign. Hence,

$$\mathcal{E}_z = C\left(Ai(-\zeta) + i\, Bi(-\zeta)\right) \qquad (34)$$

with the asymptotic forms

$$\lim_{\zeta \to \infty} \mathcal{E}_z = \frac{C}{\sqrt{\pi}\,\zeta^{1/4}} \exp -i\left(\tfrac{2}{3}\zeta^{3/2} - \tfrac{\pi}{4}\right) \qquad (38)$$

$$\lim_{\zeta \to 0} \mathcal{E}_z = \frac{2C}{3^{2/3}\,\Gamma(2/3)}\, e^{+i\pi/3} \qquad (39)$$

$$\lim_{\zeta \to 0} \frac{d\mathcal{E}_z}{d\zeta} = \frac{2C}{3^{1/3}\,\Gamma(1/3)}\, e^{-i\pi/3} \qquad (40)$$

From (19), (22), (39), and (40), we then have

$$Y_{pe}(n_z) = \frac{e^{-i\pi/6}\ \alpha^{1/3}}{z_0\ |n_z^2-1|^{2/3}}\ \frac{3^{2/3}\Gamma(2/3)}{3^{1/3}\Gamma(1/3)} \qquad |n_z|>1 \tag{41}$$

and, from (32) and (36)

$$S_{x,pe} = \frac{cc^* \alpha^{1/3}}{2\pi z_0\ |n_z^2-1|^{2/3}}$$

IV TRANSMITTED POWER TO PLASMA ; SPECTRAL POWER DENSITY

The power transferred by the kth waveguide to the plasma per unit height of the waveguide is given by :

$$S_k = -\frac{1}{2}\,\mathrm{Re}\int_{z_k-b_k/2}^{z_k+b_k/2} dz\,\left(E_z^k(0,z)\right)^* H_y^k(0,z)$$

or

$$S_k = \frac{Y_0 b_k}{2}\,\mathrm{Re}\left[(E_{ik}^*+E_{rk}^*)(E_{ik}-E_{rk})\right] \tag{42}$$

(42) may immediately be rewritten to give the expected expression for the power transmitted by the kth guide per unit height

$$S_k = \frac{Y_0 b_k}{2}\left(|E_{ik}|^2 - |E_{rk}|^2\right) \tag{43}$$

which simply means that the transmitted power is given by the difference of incident and reflected power. However, we may also substitute (6) into (42) to obtain a spectral form of the power transferred,

$$S_k = \frac{1}{2}\,\mathrm{Re}\left[\int_{-\infty}^{\infty} dn_z\, Y_{pe}(n_z)\,\mathcal{E}_z(n_z)\,(E_{ik}^*+E_{rk}^*)\,G_k^*(n_z)\right] \tag{44}$$

The total power transferred to the plasma by the entire grill per unit height is then given by

$$S = \sum_{k=1}^{\ell} S_k = \frac{1}{2}\,\mathrm{Re}\left[\int_{-\infty}^{\infty} dn_z\, Y_{pe}(n_z)\,|\mathcal{E}_z(n_z)|^2\right] \tag{45}$$

where we have substituted(4).

Using the definition

$$A \equiv \frac{3^{2/3}\,\Gamma(2/3)}{3^{1/3}\,\Gamma(1/3)}\,\alpha^{1/3} = \frac{11.42}{f_G}\,(\nabla n_{13})^{1/3} \tag{46}$$

where f_G is the frequency in GHz, ∇n_{13} is the edge density gradient in units of 10^{13} cm^{-4}, we now substitute the expressions (26) and (41) for the wave admittance of the plasma at the waveguide mouth to obtain

$$S = \frac{1}{2} Y_0 A \cos\frac{\pi}{6} \int_{|n_z|>1} \frac{dn_z\,|\mathcal{E}_z(n_z)|^2}{|n_z^2-1|^{2/3}} \tag{47}$$

There is no contribution to the integral for $|n_z| < 1$ since, from (26), $Y_{p\ell}(n_z)$ is purely imaginary for $|n_z| < 1$. The expression (4) for $\varepsilon_z(n_z)$ is here repeated for convenience :

$$\mathcal{E}_z(n_z) = \sum_{m=1}^{\ell} (E_{im} + E_{rm})\, G_m(n_z) \tag{4}$$

From (47), the spectral power density $S(n_z)$, defined from

$$S \equiv \int_{-\infty}^{\infty} dn_z\, S(n_z) \tag{48}$$

is proportional to

$$S(n_z) \propto \frac{|\mathcal{E}_z(n_z)|^2}{|n_z^2-1|^{2/3}} \tag{49}$$

From (49), we note that the spectral power density depends only on the Fourier transform of the total electric field at x = 0, which depends, from (4), only on the total field at each waveguide mouth

$$E_k \equiv E_{ik} + E_{rk} \tag{50}$$

In the sections dealing with the optimization of the power spectrum, we shall therefore consider the total electric fields E_k and the geometry of the grill to be specified, and deduce the dependence of the power spectrum on the distribution of the E_k. Once a reasonable power spectrum has been found, the distribution of the incident fields necessary to produce the distribution of total fields corresponding to the spectrum may be calculated, as shown in the next section.

V DEDUCTION OF WAVEGUIDE QUANTITIES, DENSITY DEPENDENCE

We have noted in the previous section that the total field distribution E_k at the waveguide mouths specifies completely the spectral density of power transmitted to the plasma.

We shall now deduce the waveguide parameters as a function of the density gradient in order to produce the prescribed spectrum.

We define the surface admittance of the plasma viewed from the mouth of the k[th] guide by

$$Y_k \equiv Y_0 \frac{E_{ik} - E_{vk}}{E_{ik} + E_{vk}} \tag{51}$$

From (6) and (50), this may be rewritten

$$Y_k = \frac{\sum_{m=1}^{\ell} E_m}{b_k E_k} \int_{-\infty}^{\infty} dn_z \, Y_{p\ell}(n_z) G_m(n_z) G_k^*(n_z) \qquad k = 1 \ldots \ell \tag{52}$$

We now substitute the expression for $Y_{p\ell}$ from (26) and (41), using definition (46) to obtain

$$Y_k = \frac{Y_0 A}{b_k E_k} \sum_{m=1}^{\ell} E_m \left[e^{i\pi/2} \int_{|n_z|<1} \frac{dn_z \, G_m(n_z) G_k^*(n_z)}{|1-n_z^2|^{2/3}} + e^{-i\pi/6} \int_{|n_z|>1} \frac{dn_z \, G_m(n_z) G_k^*(n_z)}{|n_z^2-1|^{2/3}} \right]$$

Substituting for $G_m(n_z) G_k^*(n_z)$, and noticing that the imaginary part of this quantity is odd in n_z, and therefore its integral is zero, we obtain

$$Y_k = \frac{Y_0 A}{b_k E_k} \sum_{m=1}^{\ell} E_m \left(e^{i\pi/2} K_{mk} + e^{-i\pi/6} I_{mk} \right) \tag{54}$$

where

$$K_{mk} \equiv \frac{4}{\pi} \int_0^1 dn_z \frac{\cos n_z (z_m - z_k) \sin \frac{n_z b_m}{2} \sin \frac{n_z b_k}{2}}{n_z^2 \, |1-n_z^2|^{2/3}} \tag{55}$$

and

$$I_{mk} \equiv \frac{4}{\pi} \int_1^{\infty} dn_z \frac{\cos n_z (z_m - z_k) \sin \frac{n_z b_m}{2} \sin \frac{n_z b_k}{2}}{n_z^2 \, |n_z^2-1|^{2/3}} \tag{56}$$

We note that K_{mk} and I_{mk} are real, and symetric in m and k.

They depend only on the geometry of the grill. As the density gradient is changed, we hold the power spectrum transmitted to the plasma constant, and hence, as shown in the previous section, hold the relative total field amplitude and phases E_k constant. Under these conditions, the magnitude of Y_k is proportional to A (and hence to $(\nabla n)^{1/3}$), while the phase of Y_k remains constant, containing, in general, a non-zero reactive susceptance.

From (51), the field reflection coefficient is simply written as

$$\rho_k \equiv \frac{E_{rk}}{E_{ik}} = \frac{1 - Y_k/Y_0}{1 + Y_k/Y_0} \tag{57}$$

Since, as a function of A, the phase of Y_k, $\underline{|Y_k}$, does not change, the mimimum reflection coefficient is obtained when

$$|Y_k| = Y_0$$

for which case

$$A = A_{k0} = \frac{b_k\,|E_k|}{\left|\sum_{m=1} E_m\left(e^{i\pi/2} K_{mk} + e^{-i\pi/6} I_{mk}\right)\right|} \tag{58}$$

and

$$\min\{|\rho_k|^2\} = |\rho_k(A_{k0})|^2 = \frac{1 - \cos \underline{|Y_k}}{1 + \cos \underline{|Y_k}} \tag{59}$$

From (59), we see that the minimum reflection coefficient can only be zero if the phase of Y_k iszero. Since this phase depends on the spectrum to be excited (see (54)), it may be zero for some guides of the grill but will, in general, never be zero for all the waveguides of a grill.

From (42), (48), and (51), the power transferred to the plasma by the k'th waveguide per unit height is written

$$S_k = \frac{b_k}{2} |E_k|^2 \,\mathrm{Re}\, Y_k \tag{60}$$

Since, from (54) and as already noted above, all the Y_k's are directly proportional to A, the fraction of the total power supplied by k^{th} waveguide to the plasma is independent of the density gradient, provided the total fields, and hence the power spectrum, are kept constant. Indeed, using (60) and (54), we may write the total power explicitly as

$$S = \sum_{k=1}^{\ell} S_k = \frac{1}{2} Y_0 A \cos\frac{\pi}{6} \sum_m \sum_k E_k^* E_m I_{mk} \tag{61}$$

where we have used the symmetry of I_{mk} and K_{mk}

This is easily seen to be equivalent to the expression (47) in the previous section.

The k^{th} power fraction may be written explicitly as

$$\frac{S_k}{S} = R_k \cos \angle Y_k \tag{62}$$

where

$$R_k \equiv \frac{|E_k| \cdot \left| \sum_{m=1}^{\ell} E_m \left(e^{i\pi/2} K_{mk} + e^{-i\pi/6} I_{mk} \right) \right|}{\sum_j \sum_m E_j^* E_m I_{mj} \cos\frac{\pi}{6}} \tag{63}$$

It is seen that this power fraction depends explicitly only on the fields and the phase of Y_k. Since $\cos \angle Y_k$ may be negative, it is seen that the power fraction may be negative, which simply reflects the fact that the power coupled into the k'^{th} guide by the other guides may be larger than the power it furnishes itself.

In the following expressions, the dependence on A (i.e. $(\nabla n)^{1/3}$) is expressed in terms of a function ζ_k

$$\zeta_k \equiv \frac{1}{2}\left(\frac{A}{A_{ko}} + \frac{A_{ko}}{A}\right) \tag{64}$$

which is symmetric in A/A_{ko} and its inverse, and is 1 for the density gradient for which the reflection coefficient is minimum. From (57), (58) and (64), we obtain the power reflection coefficient

$$|\rho_k|^2 = \frac{\zeta_k - \cos\angle Y_k}{\zeta_k + \cos\angle Y_k} \tag{65}$$

From this and (62), we deduce the incident and reflected powers, expressed as a fraction of the total power transmitted to the plasma, as

$$\frac{S_{ik}}{S} = \frac{R_k}{2}\left(\zeta_k + \cos\angle Y_k\right) \tag{66}$$

$$\frac{S_{rk}}{S} = \frac{R_k}{2}\left(\zeta_k - \cos\angle Y_k\right) \tag{67}$$

The standing wave ratio in the k^{th} waveguide is

$$\Gamma_k = \frac{1+|\rho_k|}{1-|\rho_k|} = \frac{\sqrt{\zeta_k + \cos\angle Y_k} + \sqrt{\zeta_k - \cos\angle Y_k}}{\sqrt{\zeta_k + \cos\angle Y_k} - \sqrt{\zeta_k - \cos\angle Y_k}} \tag{68}$$

Another important parameter is the ratio of maximum field in the waveguide to the nominal field in the waveguide, since this will determine the power which may actually be transmitted to the plasma for a given spectrum, if the local electric field is limited due to breakdown or multipactor effect, . Here, the k^{th} nominal field is defined as the incident field in the k^{th} waveguide which correspond to transmission of the power to the plasma at equal power density in all the guides in the absence of reflections and coupling between the waveguides.
As expected, the square of this ratio turns out to be equal to

$$Q_k \equiv \left|\frac{E_k^{max}}{E_k^{nom}}\right|^2 = \Gamma_k \frac{S_k/b_k}{S/\sum_m b_m} \tag{69}$$

i.e. the standing wave ratio times the ratio of transmitted power density in the k^{th} guide to average power density of the grill. However, in our case, the reflection coefficient may be larger than one, and the SWR infinite or negative without producing infinite fields in the k^{th} waveguide, reflecting the fact that some waveguides may be receiving net power rather than furnishing it. We therefore prefer to rewrite the quality factor of the k^{th} guide, Q_k, and of the grill Q, as

$$Q_k = \frac{R_k \sum_m b_m}{2\, b_k} \left\{ \sqrt{\zeta_k + \cos\underline{/\gamma_k}} + \sqrt{\zeta_k - \cos\underline{/\gamma_k}} \right\}^2 \tag{70}$$

$$Q \equiv \min_A \left\{ \max_k \left(Q_k\right) \right\}$$

Eq.70 for Q_k shows that the fields in the k^{th} guide do not diverge. The grill quality factor Q, the minimum as a function of A ($(\nabla n)^{1/3}$) of the largest of the Q_k, may be interpreted as the ratio of nominal (electric-field -limited) power to actual power transferred under the best conditions, and plays, in this respect, the same role for the entire grill as the SWR would for a single waveguide.

We note that all the quantities (65) to (70) depend on the density gradient only via the symetric function ζ_k. Hence all these quantities have a minimum for $A = A_{ko}$, and are mirror-symmetric about this point when plotted as a function of $\log A/_{A_{ko}}$. This comes about only because we have specified the total field distribution, rather than the incident field distribution to be constant.

It remains to calculate the phases of the incident and reflected fields relative to the phase of the total field (which is the major factor in determining the power spectrum and is therefore specified, rather than deduced.

From (57) and (58), the phase of the incident field is given by ($\underline{/E_k}$ is the phase of the total field $E_k = E_{ik} + E_{rk}$)

$$\underline{/E_{ik}} = \underline{/E_k} + \tan^{-1} \frac{\frac{A}{A_{ko}} \sin\underline{/\gamma_k}}{1 + \frac{A}{A_{ko}} \cos\underline{/\gamma_k}} \tag{71}$$

and the phase of the reflected field is

$$\angle E_{rk} = \angle E_k + \tan^{-1}\frac{-\frac{A}{A_{ko}}\sin\angle Y_k}{1-\frac{A}{A_{ko}}\cos\angle Y_k} \qquad (72)$$

The phase of the reflection coefficient is

$$\angle \rho_k = \angle E_{rk} - \angle E_{ik} = \tan^{-1}\frac{-\sin\angle Y_k}{-\frac{1}{2}\left(\frac{A}{A_{ko}} - \frac{A_{ko}}{A}\right)} \qquad (73)$$

The above expressions have been written so as to permit deduction of the correct quadrant from the signs of numerator and denominator. For positive $\angle Y_k$, $\angle \rho_k$ goes from 0 via $-\pi/2$ at $A = A_{ko}$ to π as A goes from 0 to infinity. For negative $\angle Y_k$ (the more usual case since, as can be seen by inspection of (54), $\angle Y_k$ would be $-\pi/6$ in the absence of contributions from $0<|n_z|<1$), $\angle \rho_k$ goes from 0 via $+\pi/2$ at $A=A_{ko}$ to π as A goes from zero to infinity. We see that the plasma passes from an open circuit at low density gradients to a short circuit at high density gradients, as expected.

VI- SPECTRAL POWER DENSITY OF MULTIWAVE GUIDE GRILLS

A major concern of lower hybrid experiments is the design of grills coupling only a small fraction of the power into the inaccessible tion of the spectrum ($1 < |n_z| < |n_{za}|$, where N_{za} is, for the case of WEGA, of the order of 1.8), in order to maximize the heating power in the central portion of the plasma and to reduce the unused power which may lead to unwanted effects (impurity influx, density increase, wall heating in multi-MW experiments). One method of reducing this power has been proposed (Ref. 7) for the case of the classical 4-element grill. The method amplitude modulation consists in reducing the incident power in the outer waveguides to 1/4 of the incident power in the inner waveguides. While the inaccessible power is reduced almost to zero for this special case, the results are not necessarily as strinkingfor a grill of more than 4 waveguides, and, if one assumes that the total power transferrable per waveguide is limited (by , for example, the multipactor effect), the total power transferrable through the grill opening is reduced to 63% the possible value.

With these considerations in mind, we shall now proceed to investigate the dependence on n_z of the spectral power density $S(n_z)$ given in (49), specifying the total electric fields at the waveguide mouths in accordance with the remarks in Section IV. We shall separate the effects of grill geometry from the effects of the distribution of field amplitudes and phases to synthesize a reasonable power spectrum. For convenience, we define the normalized " geometrical spectrum "

$$P(n_z) \equiv \frac{|\mathcal{E}_z(n_z)|^2}{\int_{-\infty}^{\infty} dn_z \, |\mathcal{E}_z(n_z)|^2} \qquad (74)$$

in terms of which (49) is written

$$S(n_z) = \frac{1}{2} Y_0 A \cos\frac{\pi}{6} \left(\sum_k |E_k|^2 b_k \right) \frac{P(n_z)}{|n_z^2 - 1|^{2/3}}, \quad |n_z| > 1 \qquad (75)$$

$$= 0 \qquad |n_z| < 1$$

where we have used Parseval's Theorem

$$\int_{-\infty}^{\infty} dn_z \, |\mathcal{E}(n_z)|^2 = \int_{-\infty}^{\infty} dz \, |E(0,z)|^2 = \sum_{k=1}^{\ell} |E_k|^2 b_k$$

Hence, aside from the weight factor $|n_z^2 - 1|^{2/3}$, due to the plasma, $P(n_z)$ contains all the information about the structure of the spectrum. Since we normally demand a spectrum with a well-defined peak, the grill configurations chosen must possess a high degree of symmetry. Three such configurations are studied below.

a) " Odd and " Even " Standing-Wave Grills

We consider grill configurations in which the total electric field has l_p complete periods of normalized length p (pspace = $2\pi \frac{p}{b}$). To produce a standing wave, all waveguides composing this electric field must have relative phases of either 0 or π. We distinguish two special cases : the " odd " grill, in which the electric field is left-right antisymmetric about the center of the grill, and the " even " grill, whose field is left-right symmetric. In each quarter-period, the field is specified according to Table I, where z is measured from the center of the grill.

TABLE I

z	$E_{odd}(0,z)$	$E_{even}(0,z)$
$-\frac{p}{2} < z < -\frac{p}{4}$	$-E_0 h(-\frac{p}{4}-z)$	$-E_0 h(z+\frac{p}{2})$
$-\frac{p}{4} < z < 0$	$-E_0 h(z+\frac{p}{4})$	$E_0 h(-z)$
$0 < z < \frac{p}{4}$	$E_0 h(\frac{p}{4}-z)$	$E_0 h(z)$
$\frac{p}{4} < z < \frac{p}{2}$	$E_0 h(z-\frac{p}{4})$	$-E_0 h(\frac{p}{2}-z)$
Other z	$E(0,z) = E(0, z \pm k\ell_p)$	

(76)

Here, h (z) is considered to be positive for $0 < z < p/4$. It is seen that the above fields are constructed by folding the field of the preceding quarter period successively about the E and z axes. The odd grill has the structure of sin (n_{zp}), the even grill of cos (n_{zp}), and both may therefore be expected to give a strong peak at $n_{zp} = 2\pi/p$.

The Fourier transform of the electric field is

$$\left\{\begin{matrix} |E_{odd}(n_z)| \\ |E_{even}(n_z)| \end{matrix}\right\} = \frac{2}{\sqrt{2\pi}} E_0 \left| \sum_{k=1}^{\ell_p} (-1)^{k+1} \cdot 2\sin\left((2k-1)\frac{n_z p}{4}\right) \right| \int_0^{p/4} du\, h(u) \cdot \left\{\begin{matrix} \cos n_z u \\ \sin n_z(\frac{p}{4}-u) \end{matrix}\right\} \tag{77}$$

and the " geometrical spectrum " P (n_z) is, from (74), using Parseval's Theorem and performing the sum in (77).

$$\left\{\begin{matrix} P_{odd}(n_z) \\ P_{even}(n_z) \end{matrix}\right\} = \frac{\sin^2 \frac{\ell_p n_z p}{2}}{2\pi \ell_p \cos^2 \frac{n_z p}{4}} \frac{\left[\int_0^{p/4} h(u) \left\{\begin{matrix} \cos n_z u \\ \sin n_z(\frac{p}{4}-u) \end{matrix}\right\} du\right]^2}{\int_0^{p/4} h^2(u)\, du} \tag{78}$$

The " odd" grill is the classical grill, composed of, for example, an even number of elements, with equal amplitudes, and phases of 0 and π or equal groups of 0 and π.

As a specific example, the classical 4-element grill with vanishing wall thickness and phases 0,π, 0,π has

$$\ell = 4, \quad lp = 2, \quad h(x) = 1, \quad b = p/2$$

For this grill, the geometrical spectrum is, from (78)

$$P_{odd,4}(n_z) = \frac{1}{2\pi b n_z^2} \frac{\sin^2 2n_z b}{\cos^2 \frac{n_z b}{2}} \sin^2 \frac{n_z b}{2}$$

The " even " grill is a novel arrangement to produce a standing wave at the same basic n_z as the corresponding " odd"grill.
If the corresponding " odd " grill was produced by grouping the waveguides in groups of two (0,0, π ,π, etc.) the corresponding " even " grill is produced by shifting the phases (0, π π, 0, etc..). If the " odd " grill was composed of single waveguides, the corresponding " even " grill is produced by taking one-half of the last waveguide from the left side and placing it on the right (at constant electric field and phase, i.e.- half power). In the last configuration, the " even " grill is therefore composed of an odd number of full-width waveguides plus two half-width waveguides.

As an example of the even analogue to the 4-element grill, we define a 5-element grill having widths b/2 : b : b : b : b/2,

equal electric field amplitudes, phases 0 : π: 0 : π : 0, and powers $\frac{1}{2} : 1 : 1 : 1 : \frac{1}{2}$. Then

$$\ell = 5, \quad lp = 2, \quad h(x) = 1, \quad b = p/2$$

Hence, from (78)

$$P_{even,5}(n_z) = \frac{1}{2\pi b n_z^2} \frac{\sin^2 2n_z b}{\cos^2 \frac{n_z b}{2}} \left[1 - \cos\frac{n_z b}{2}\right]^2$$

b) The " Travelling Wave " Grill

This grill configuration produces an asymmetric spectrum, $P(n_z) \neq P(-n_z)$. While the asymmetry is of great interest to produce RF- driven current (Ref. 12,13) the possibility of dynamic tailoring of the n_z spectrum by changing the phase difference from one guide to the next also makes this arrangement very attractive.

We shall assume that the electric field amplitudes are repeated every period P_ϕ, that from one period to the next the phase is advanced by ϕ, and that there are ℓ_ϕ such periods, i.e.

$$E(0,z) = E_0\, h_\phi(z) \qquad 0 < z < P_\phi$$

$$E(0,z) = E\left(0,\tfrac{z}{k}\right) e^{ik\phi}, \text{ other } z, \text{ where } k \text{ is an integer such that } 0 < \tfrac{z}{k} < P_\phi \tag{79}$$

The Fourier transform of the electric field is then given by

$$\mathcal{E}_\phi(n_z) = \frac{1}{\sqrt{2\pi}}\, E_0\, \frac{\cos \ell_\phi(\phi - n_z P_\phi) - 1 + j \sin \ell_\phi(\phi - n_z P_\phi)}{\cos(\phi - n_z P_\phi) - 1 + j \sin(\phi - n_z P_\phi)} \cdot \int_0^{P_\phi} h_\phi(u)\,(\cos n_z u - j \sin n_z u) \tag{80}$$

and

$$P_\phi(n_z) = \frac{1}{2\pi \ell_\phi}\, \frac{\sin^2 \ell_\phi \frac{\phi - n_z P_\phi}{2}}{\sin^2 \frac{\phi - n_z P_\phi}{2}} \cdot \frac{\left[\int_0^{P_\phi} h_\phi(u) \cos n_z u\, du\right]^2 + \left[\int_0^{P_\phi} h_\phi(u) \sin n_z u\, du\right]^2}{\int_0^{P_\phi} h_\phi^2(u)\, du} \tag{81}$$

This expression may be simplified if h (z) has left-right symmetry within the period P_ϕ, which we shall assume in the following. Then $h_\phi(P_\phi - z) = h_\phi(z)$ and we have

$$P_\phi(n_z) = \frac{1}{2\pi \ell_\phi}\, \frac{\sin^2 \ell_\phi \frac{\phi - n_z P_\phi}{2}}{\sin^2 \frac{\phi - n_z P_\phi}{2}} \cdot \frac{\left[\sqrt{2} \int_0^{P_\phi/2} h_\phi(u) \cos n_z \left(u - \frac{P_\phi}{2}\right) du\right]^2}{2\int_0^{P_\phi/2} h_\phi^2(u)\, du} \tag{82}$$

We note in passing that we obtain the same expression as for the odd standing wave grill if we set

$$P_\phi = p/2, \quad l_\phi = 2 l_p, \quad \phi = \pi, \quad h_\phi(x) = h(p/4 - x)$$

as expected.

We now consider the particular case where $\phi=\pi/2$. Setting

$$P_\phi = P/4 \,, \quad \ell_\phi = 4\ell_p \,, \quad \phi = \pi/2 \,, \quad h_\phi(z) = h_\phi(p/4 - z)$$

We find, for this particular case

$$P_{\pi/2}(n_z) = \frac{1}{2\pi \ell_p} \frac{\sin^2 \frac{\ell_p n_z P}{2}}{(1-\sin \frac{n_z P}{4})} \frac{\left[\int_0^{P/4} h(u) \cdot \frac{1}{\sqrt{2}} \cos n_z (u - P/8) du \right]^2}{\int_0^{P/4} h^2(u) du} \tag{83}$$

which is, as expected, not symmetric in n_z While this expression gives the spectral power density for positive or negative n_z, it is, for comparison purposes with the " even " and " odd " grills, interesting to define an average spectral power density

$$P_{\langle\pi/2\rangle}(n_z) = \frac{1}{2} \left(P_{\pi/2}(n_z) + P_{\pi/2}(-n_z) \right)$$

Then

$$P_{\langle\pi/2\rangle}(n_z) = \frac{1}{2\pi \ell_p} \frac{\sin^2 \frac{\ell_p n_z P}{2}}{\cos^2 \frac{n_z P}{4}} \cdot \frac{\left[\int_0^{P/4} h(u) \cdot \frac{1}{\sqrt{2}} \cos n_z (u - \frac{P}{8}) du \right]^2}{\int_0^{P/4} h^2(u) du} \tag{84}$$

This is the final expression, to be compared with the analogous expressions for the two standing-wave grills.

Before leaving this topic, however, we remark that not all of this power is available, in principle, for current production by one-sided electron Landau damping (Ref. 12,13).

In fact, the part of the power which may produce current is given by

$$P^{I}_{\pi/2}(n_z) = P_{\pi/2}(n_z) - P_{\pi/2}(-n_z) \tag{85}$$

or $$P^{I}_{\pi/2}(n_z) = 2 \sin \frac{n_z p}{4} P_{\langle\pi/2\rangle}(n_z) \qquad (86)$$

Since this expression can charge sign, current produced in one part of the spectrum can, in principle, be reduced by an opposing current in another part of the spectrum although in practice, conditions on the ratio of phase to thermal velocity (optimum n_z for current production) will tend to reduce this effect.

c) Comparison of the three grill types

The spectral density of transmitted power S (n_z) may be written for the three grill types as, from (75), (78), and (84)

$$S(n_z) = \frac{1}{2} Y_0 A \cos\frac{\pi}{6} \left(\sum_{k=1}^{\ell} |E_k|^2 b_k\right) \cdot \frac{\alpha(n_z, \ell_p, n_{zp}) \cdot \beta(h(z), n_z, n_{zp})}{n_{zp} |n_z^2 - 1|^{2/3}} \qquad (87)$$

$$= 0 \quad |n_z| < 1$$

where α is a function depending only on the number of periods and the size of the period chosen but not on the grill configuration, β depending on the type of grill configuration (even, odd, $\pi/2$), and the distribution of waveguides inside each quarter-period, but not on the number of periods. We may therefore separate the effects of grill length and grill configuration by studying each term separately. α, β, and n_{zp} are defined below.

d) The periodicity function α (n_z, l_p, n_{zp})

The function α is defined as

$$\alpha(n_z, \ell_p, n_{zp}) \equiv \frac{1}{\pi^2 \ell_p} \frac{\sin^2 \ell_p \pi \frac{n_z}{n_{zp}}}{\cos^2 \frac{\pi}{2} \frac{n_z}{n_{zp}}} \qquad (88)$$

where (89)

$$n_{zp} \equiv \frac{2\pi}{p} = \frac{\lambda_0}{p_{space}}$$

is the principal parallel wavenumber corresponding to the chosen period p.

α is the same for all three grills, depending on n_z, the number of periods, and the length of each period. In Fig. 1 , α is plotted for the case of 1, 2, and 4 periods.

α contains the basic distribution of zeroes and peaks of the power spectrum. In fact, it is easily seen that α has zeroes at

$$n_z = n_{zp}\left(2m+1 \pm \frac{k}{\ell_p}\right) \qquad m = 0, \pm 1, \ldots \quad k = 1, 2, \ldots, \ell_p \tag{90}$$

and major peaks for zeroes of the denominator

$$n_z = n_{zp}(2m+1) \qquad m = 0, \pm 1, \ldots \tag{91}$$

Because of the strong damping of higher n_z's by the function β, only the first of these major peaks, $m = 0$, $n_z = n_{zp}$, is important. Hence, the principal peak of α is given only by the period

$$n_{zp} = \frac{2\pi}{p} = \frac{\lambda}{p_{space}} \tag{92}$$

i.e. ratio of wavelength to period in non-normalized dimensions. The height of this peak is given by

$$\alpha(n_{zp}) = \frac{4\ell_p}{\pi^2} \tag{93}$$

The width of the principal peak is given by the distance between zeroes

$$\Delta n_z\big|_p = \frac{2n_{zp}}{\ell_p} = \frac{2\lambda}{\ell_p\, p_{space}} = \frac{2\lambda}{L_{space}} \tag{94}$$

If we recognize that $L = l_p$ pspace is nothing but the total length of the grill, we see that the width of the principal peak depends only on the ratio of the wavelength to the total length of the grill, and not on the number of periods inside the length,

(95)

The secondary peaks of α are only half as wide as the principal peak

$$\Delta n_z|_S = \frac{n_{zp}}{\ell_p} = \frac{\lambda}{L_{space}} \tag{96}$$

They are centered on

$$n_{zs,k} = n_{zp}\left(2m+1 \pm \frac{k+\frac{1}{2}}{\ell_p}\right) \quad m=0,\pm 1,\dots \quad k=1,2,\dots,\ell_p-1 \tag{97}$$

The amplitude of the k^{th} secondary peak is given by

$$\alpha(n_{zs,k}) = \frac{1}{\pi^2 \ell_p \sin^2 \frac{\pi}{2}\frac{k+\frac{1}{2}}{\ell_p}} \quad k=1,2,\dots,\ell_p-1 \tag{98}$$

The secondary peaks therefore decrease in amplitude away from the primary peak. The ratio of the amplitude of the first secondary peak ($n_{zs,1} = n_{zp} \pm \frac{3}{2Tp}$) to the primary peak is given by

$$\frac{\alpha(n_{zs,1})}{\alpha(n_{zp})} = \frac{1}{4\ell_p^2 \sin^2 \frac{3\pi}{4\ell_p}} \quad [\ell_p > 1] \tag{99}$$

As the number of periods becomes large, $lp \gg \frac{3\pi}{4}$, this ratio goes to a constant value.

$$\lim_{\ell_p \gg \frac{3\pi}{4}} \frac{\alpha(n_{zs,1})}{\alpha(n_{zp})} = \frac{4}{9\pi^2} = 4.5\% \tag{100}$$

Hence, while increasing the length of the grill narrows the width of the principal peak, the quality, i.e. the ratio between the amplitudes of the principal and secondary peaks, can not be improved be yond a certain point. Here, the structure of the function β becomes important.

e) The configuration function β (n_z, n_{zp}).

From (75), (78), (84), (87), and (88), the function β may be written for the three grill configurations under consideration.

$$\beta_{odd}(n_z, n_{zp}) = \frac{\pi^2}{p} \frac{\left[\int_0^{p/4} h(u) \cos n_z u \, du\right]^2}{\int_0^{p/4} h^2(u) du} \tag{101}$$

$$\beta_{even}(n_z, n_{zp}) = \frac{\pi^2}{p} \frac{\left[\int_0^{p/4} h(u) \sin n_z \left(\frac{p}{4} - u\right) du\right]^2}{\int_0^{p/4} h^2(u) du} \tag{102}$$

$$\beta_{\langle\pi/2\rangle}(n_z, n_{zp}) = \frac{\pi^2}{p} \frac{\left[\int_0^{p/4} h(u) \cdot \frac{1}{\sqrt{2}} \cos n_z \left(u - \frac{p}{8}\right) du\right]^2}{\int_0^{p/4} h^2(u) du} \tag{103}$$

where $n_{zp} = \frac{2\pi}{p}$

From the above equations, we see immediately that, for $n_z = n_{zp} = \frac{2\pi}{p}$ (and $h(u)$ having left-right symmetry in the quarter-period)

$$\beta_{odd} = \beta_{even} = \beta_{\langle\pi/2\rangle} = \frac{\pi^2}{p} \frac{\left[\int_0^{p/4} h(u) \cos \frac{2\pi u}{p} du\right]^2}{\int_0^{p/4} h^2(u) du} \tag{104}$$

i.e. the three configurations give the same total spectral density (not necessarily the maximum) at the center of the principal peak.

Furthermore, we note that, for all $n_z \leq n_{zp} = \frac{2\pi}{p}$

$$\sin n_z \left(\frac{p}{4} - u\right) \leq \cos n_z u \quad ; \text{all} \quad 0 \leq u \leq \frac{p}{4} \tag{105}$$

Hence,

$\beta_{even} \leq \beta_{odd}$ for all $n_z \leq n_{zp}$

Hence we have proved that the "even" grill has a lower spectral power density than the " odd " grill for all parallel wavenumbers less than the principal n_z, and therefore has, in particular, a smaller nonaccessible power. If, in addition, we impose the not very stringent condition of left-right symmetry on h (z) i.e.

$$h\left(\frac{P}{4}-z\right) = h(z) \tag{107}$$

we obtain a universal form for the configuration function for the three cases, i.e.

$$\beta(n_z, n_{zp}) = \gamma \cdot \frac{\pi^2}{P} \frac{\left[\int_0^{P/4} h(u)\cos n_z \left(u-\frac{P}{8}\right)du\right]^2}{\int_0^{P/4} h^2(u)du} \tag{108}$$

where

$$\gamma_{odd} = \cos^2 \frac{n_z P}{8} = \cos^2 \frac{\pi}{4}\frac{n_z}{n_{zp}}$$

$$\gamma_{\langle\pi/2\rangle} = \frac{1}{2} = \cos^2\frac{\pi}{4} \tag{109}$$

$$\gamma_{even} = \sin^2 \frac{n_z P}{8} = \sin^2 \frac{\pi}{4}\frac{n_z}{n_{zp}}$$

From these expressions, it is clear that

$$\beta_{even} < \beta_{\langle\pi/2\rangle} < \beta_{odd} \quad \text{for } \underline{\text{all}} \quad 0 \le n_z \le n_{zp}$$

i.e. the travelling-wave case is better than the odd case, and not as good as the even case. As n_z goes to zero

$$\beta_{even} : \beta_{\langle\pi/2\rangle} : \beta_{odd} = 0 : 1/2 : 1$$

i.e. the power density of the even grill goes to zero at low n_z.

f) Equal-Amplitude, Equally-Spaced Waveguides

The above expressions many be written explicitly if each quarter-period (108) and (109) is composed of a number l_w of equal-spacing, equal-amplitude waveguides.

Let the total number of waveguides be

$$\ell = 4 l_w l p \tag{110}$$

where l_w is the number of waveguides per quarter-period and l_p is the number of periods as before. Let the width (normalized to $\lambda_0/2\pi$) of each waveguide be given by b, the spacing by $z_w = \frac{p}{4 l_w}$, and let the waveguides be centered at

$$z_k = \frac{p}{8 l_w},\ \frac{3p}{8 l_w},\ \ldots,\ \frac{(2 l_w - 1)p}{8 l_w} \qquad 0 < z < \frac{p}{4} \tag{111}$$

The wall thickness is, of course, given by

$$t = \frac{p}{4 l_w} - b \geq 0 \tag{112}$$

Then, with $n_{zp} = {}^{2\pi}/p$ as before, and the " filling factor " (ratio of waveguide area to total area occupied by the grill) defined as

$$F = \frac{l_w b}{p/4} \tag{113}$$

we may rewrite

$$\beta(n_z, n_{zp}) = \beta_F \cdot \beta_c \tag{114}$$

where β_F is a factor common to all three grill types and depends on the filling factor :

$$\beta_F = \frac{\sin^2 F \frac{\pi}{4 l_w} \frac{n_z}{n_{zp}}}{F \sin^2 \frac{\pi}{4 l_w} \frac{n_z}{n_{zp}}} = \frac{\sin^2 \frac{n_z b}{2}}{F \sin^2 \frac{\pi}{4 l_w} \frac{n_z}{n_{zp}}} \tag{115}$$

and β_c depends on the configuration :

$$\beta_{c,odd} = \frac{\sin^2 \frac{\pi}{2} \frac{n_z}{n_{zp}}}{(n_z/n_{zp})^2}$$

$$\beta_{c,(\pi/2)} = \frac{1 - \cos \frac{\pi}{2} \frac{n_z}{n_{zp}}}{(n_z/n_{zp})^2} \tag{116}$$

$$\beta_{c,\text{even}} = \frac{\left(1-\cos\frac{\pi}{2}\frac{n_z}{n_{zp}}\right)^2}{(n_z/n_{zp})^2}$$

This configuration factor is plotted for the three types of grills as a function of n_z/n_{zp} in Fig. 2. As expected, all three are equal at $n_z = n_{zp}$, and, as $n_z \to 0$, they scale as

$$\lim_{n_z\to 0} \beta_{\text{even}} : \beta_{(\pi/2)} : \beta_{\text{odd}} = \frac{\pi^4}{64}\frac{n_z^2}{n_{zp}^2} : \frac{\pi^2}{8} : \frac{\pi^2}{4}$$

It is worth while to write down the explicit expression for the power spectrum for the case of equal-amplitude, equally spaced waveguides treated here. From (87), (88), (115), and (116), it is given by

$$\begin{Bmatrix} S_{\text{odd}}(n_z) \\ S_{(\pi/2)}(n_z) \\ S_{\text{even}}(n_z) \end{Bmatrix} = \frac{1}{2} Y_0 A \cos\frac{\pi}{6}\, |E|^2 \cdot \frac{2}{\pi} \cdot \frac{\sin^2 l_p \pi \frac{n_z}{n_{zp}} \sin^2\frac{n_z b}{2}}{n_z^2\, |n_z^2-1|^{2/3} \sin^2\frac{\pi}{4 l_w}\frac{n_z}{n_{zp}} \cdot \cos^2\frac{\pi}{2}\frac{n_z}{n_{zp}}} \cdot \tag{117}$$

$$\cdot \begin{Bmatrix} \sin^2\frac{\pi}{2}\frac{n_z}{n_{zp}} \\ 1-\cos\frac{\pi}{2}\frac{n_z}{n_{zp}} \\ \left(1-\cos\frac{\pi}{2}\frac{n_z}{n_{zp}}\right)^2 \end{Bmatrix}$$

where $|E|$ is the total oscillating field amplitude at the mouth of each guide and $\sin^2(n_z b/2)$ cancels against $\sin^2(\pi n_z/4 l_w n_{zp})$ when the filling factor is 1, i.e. the walls are infinitesimally thin.

To summarize this section, we have shown, for the special case of equal total field amplitudes (which does not correspond to the case of equal powers transmitted), that the basic structure of peaks and zeroes is given by the chosen periodicity and length of the grill, with a superimposed modulation depending on the grill configuration. Of the three grill configurations studied, the classical " odd " grill is seen to be the one which will tend to lose the most power in the inaccessible region, while a novel arrangement, the " even " grill, is expected to be the best in this respect.

In the examples treated numerically in the subsequent sections, we shall be forced to abandon the condition of equal oscillating field amplitude which permitted us to find simple analytical expressions above because of the large disparity of the power fractions transferred for this case, but shall retain the notions of odd and even as concerns the phases. We shall find that all the qualitative conclusions of this section are preserved.

g) Spectrum Tailoring by Phase Shift

Before leaving the idealized models developed in this section, we would like to point out another way of looking at the travelling-wave grill which will make clear the effect of changing the phase. Consider, as in section b), l_ϕ to be the number of groups of equal-phase waveguides of length p_ϕ and $\emptyset$ the phase between one group and the preceding group. Then, from (82), and (101)

$$S_\phi(n_z) = C \frac{\alpha_\phi(n_z)\,\beta_{odd}(n_z)}{|n_z^2-1|^{2/3}} \tag{118}$$

where

$$\alpha_\phi(n_z) = \frac{2}{\pi^2 l_\phi} \frac{\sin^2 \frac{l_\phi \pi}{2}\left(\frac{n_z}{n_G} + (1-\frac{\phi}{\pi})\right)}{\cos^2 \frac{\pi}{2}\left(\frac{n_z}{n_G} + (1-\frac{\phi}{\pi})\right)} \tag{119}$$

and we set, when $\emptyset = \pi$, $l_p = \frac{l_\phi}{2}$, so that $\alpha_\pi(n_z)$ is identical to the periodicity function α defined in (88) when $\emptyset = \pi$. We also define the geometrical peak n_G as

$$n_G \equiv \frac{\pi}{p_\phi} = n_{zp,\pi} \tag{120}$$

i.e. the principal peak of the spectrum when the phase is π.

From (119), we see that the effect of imposing a phase other than π is simply to translate the entire spectrum. For example, if $\emptyset < \pi$, the principal peak for positive n_z values is moved to $n_{zp} = n_G \frac{\pi-\phi}{\pi}$, i.e. closer to zero, and the negative peak is moved by the same amount away

from zero. Since the other factors in (119) are unaffected by this translation, the positive n_z peak, what is closer to zero, will increase in amplitude, and the negative peak will be damped.
When $\phi = \pi/2$, $|n_{zp}^-| = 3\,|n_{zp}^+|$, i.e. the negative peak is strongly damped.
However, when the phase is close to π, the negative peak is only weakly damped. For the purposes of tailoring the spectrum by moving the principal peak, we conclude from these consideration that dynamic tailoring can be performed for ϕ between 0 and about $\pi/2$, but not when ϕ is near π since then too much power will be lost to the second travelling wave at higher (but negative) n_z. One consequence of this conclusion is that a grill which is to be used to follow the evolution of the plasma parameters by changing the relative phase during the shot must be designed such that the " geometrical " n_G is roughly twice as high as the highst n_{zp} to be used in practice, i.e. be composed of twice as many waveguides half as large. These qualitative conclusions will be substantiated by an example in a subsequent section.

VII- IDEALIZED EXAMPLES WITH INFINITELY THIN WAVEGUIDE WALLS

In this section, we consider the power spectra of four grills, the odd 2-element grill G2 and its even 3-element analogue G3, and the odd 4-element grill G4 and its even 5-element analogue G5. The full-width waveguides of the even grills have been chosen to be 14% wider than the corresponding odd grills to compensate the fact that, for equal widths, the configuration factor of the even grill shifts the real maximum of the principal peak to a value above n_{zp} and of the odd grill to a value below n_{zp}. The phase shift of the total fields from one waveguide to the next is π.

Initially, we take equal total fields in all the waveguides. Both the spectral density, normalized to the total power transferred (full line) and its integral from 1 to n_z (dotted line) are plotted in fig. 3 and 4. Its is seen that the 2-element grill G2 ($\frac{L}{\lambda}$ = 0,25) and G3 ($\frac{L}{\lambda}$: 0,286) both have the wide spectrum expected for such short lengths from the considerations in the preceding section, but that the " even " G3 already shows a pronounced maximum near the desired n_z of 3.5, and couples 83% of the power between accessibility (here considered to be n_{za} = 1.8) and the first zero, where as G2 only couples 53% in this region, and loses 46% for $1 \leq n_z < 1.8$. The comparison between the odd G4 ($L/\lambda = 0.5$) and the even G5($L/\lambda = 0.57$) is equally striking, G4 coupling only 58% of the power into the principal peak above $n_z = 1.8$, while G5 attains 90%.

However, when the power fraction transferred by each waveguide is calculated for this situation from (62), it is seen that the prescription of equal total field does not correspond to a real experimental situation. The power fractions are given in table II, where the nominal values are simply proportional to the waveguide width.

TABLE II : POWER FRACTIONS AT EQUAL FIELD

	Guide 1		Guide 2		Guide 3		Guide 4		Guide 5	
Grill	Real	Nominal	Real	Nominal	Real	Nominal	Real	Nominal	Real	Nominal
odd G2	0.5	0.5	0.5	0.5						
even G3	0.058	0.250	0.884	0.50	0.058	0.25				
odd G4	0.481	0.250	0.019	0.250	0.019	0.250	0.481	0.250		
even G5	0.081	0.125	0.338	0.25	0.161	0.25	0.338	0.25	0.081	0.125

In G2, both guides transfer equal power by symmetry. For more waveguides, it is seen that the even grills G3 and G5 transfer less power on the outside guides than on the inside ones, while the converse is true for G4.

In order to calculate a more realistic situation, we shall now keep the same grill dimensions and phases of the total field as above, but calculate the spectral power density by setting the density of power transferred by each waveguide equal, i.e. power fraction S_k/S proportional to width.

Total field amplitudes corresponding to this prescription are calculated numerically from (62) together with (54). The resulting spectral power densities, normalized to total power, are plotted (Fig.5 and 6), as are the corresponding integrals from 1 to n_z, where we refer to these cases as G2' to G5'. Of course G2' is the same as G2 because of symmetry. Grill G3' (L/λ = 0.286) gives excellent results in spite of its short length, transferring 91.4% of the power in the principal peak and losing only 2.4% for $1<|n_z|<1.8$ Grill G4' ($\frac{L}{\lambda}$ = 0.5) is considerably better than before (Sprinc.= 87.6%, S $(1 <|n_z|<1.8)$ = 10.6%), but, as far as inaccessible power is concerned, not as good as G3' which is much shorter. Grill G5' ($\frac{L}{\lambda}$ = 0.57), the best with 91.5% of the power transferred in the principal peak, and only 1% between 1 and 1.8. Once again, the even grill configuration appears to be, from this point of view, preferable. The amazingly good results of grill G3' ($b_1 : b_2 : b_3$ = 1/2 : 1 : 1/2) may well be of interest for experiments in which the access ports are very narrow, of the order of half a wavelength.

The quality factor Q, defined in (70) as the best ratio of nominal power to transferred power, is found to be 1.55 for G2, 2.61 for G3', 2.12 for G4', and 2.47 for G5', i.e. the two-element grill can transfer the largest power density, while the other three grills are roughly equivalent.

VIII-GRILL EXAMPLES WITH FINITE WALLS

In this section, wa consider realistic examples of grills with finite wall thickness between waveguides. In all cases, we shall specify the amplitude and phase distribution of the total field in order to keep the power spectrum invariant with density gradient (Sec.IV). All the waveguide quantities are calculated according to the formulation of Sec. V.

a) Realistic 4-Waveguide Grill (WEGA)

We shall now examine in detail the results for a four-waveguide grill designed for WEGA which will be put into operation in early 1980. The frequency to be used is 800 MHz. Grill dimensions are : waveguide width 3.5 cm (b= 0.586), mean separation of waveguides 5.4 cm ($p_\pi = \Delta z$ = 0.905), 1 = 4, geometrical wavenumber (Eq.120 or 103) n_G= 3.47. Total length $L/\lambda o$ = 0.58. The wavenumber for accessibility is n_{za} = 1.8.

Since, given the above dimensions, the first zero of the major peak already lies in the inaccessible region, reduction of the n_z by changing the phasing is not productive. Accordingly, all the following curves for this grill are calculated for phases of the total field of 0, π, 0, π.

In Fig. 7, we plot the quality factors of the outside waveguides (Q_1 and Q_4) and of the inside waveguides (Q_2 and Q_3) as a function of the density gradient, for the case in which all the waveguides transfer equal power.It is seen that, under this condition, the transferrable power is limited by the inside waveguides. The minimum value of $Q_2 = 2.4$ is attained for $\nabla n = 7.2.10^{11} f_G^3 = 3.7.10^{11} cm^{-4}$. The power reflection coefficients of each waveguide as well as the global reflection coefficient $R \equiv \Sigma S_{kr}/\Sigma S_{ki}$ are plotted in the same figure.

In Fig. 8, we show the results as a function of the ratio of power transferred by the outside waveguides to that transferred by the inside waveguides, taken at $\nabla n = 6.7.10^{11} f_G^3 = 3.4.10^{11} cm^{-3}$, which is close to minimum reflection. All the powers are normalized to S, the total power transferred to the plasma. The reflected power is not directly plotted, but is simply the difference between incident power (e.g; $(S_{i2} + S_{i3})/S$) and transfered power (e.g. $(S_1 + S_2)/S$). It is seen that, when the power level of the outside waveguides is reduced ($S_1/S_2 < 1$) , the total reflected power ($\Sigma S_{ik}/S-1$) is lower. Except at the highest values of S_1/S_2, the reflected power comes mainly from the inside waveguides. When $S_1/S_2 = 0.42$, both inside and outside waveguides have their minimum reflection at the same density gradient, In addition, we plot S_{acc}/S, the ratio of useful power, between $n_z = 1.8$ and 5.5, to total power. It is seen that 95% of the power is accessible when $S_1/S_2 \leq 0.5$. For the WEGA experiment, serious electric field limitations are not expected at the presently envisaged power levels, so that, from the standpoint of reduction of inaccessible power and reflected power, the best operating regime is $S_1/S_2 \doteq 0.2 - 0.5$ While not optimal, operation at $S_1 = S_2$ remains acceptable.

For reference, the quality factors are plotted as a function of S_1/S_2 in the same figure, at $\nabla n = 6.7.10^{11} f_G^3 \ cm^{-4}$. For $S_1/S_2 < 2$, the inside waveguides will limit the transferrable power in the case of electric field limitation. We have also plotted the ratio of Q_{max} to the useful power fraction, i.e. the ratio of nominal power in the absence of reflections to useful power transferrable. At low S_1/S_2, this curve is reasonably flat, showing that reduction of the inaccessible power by decreasing the power levels of the outside waveguides does not lead to a significant reduction of the useful transferrable power.

In Fig. 9, spectral power density, normalized to total power transferred, and its integral from to n_z are plotted for two cases, $S_1/S_2 = 1$ (equal power density) and $S_1/S_2 = 0.42$ (All waveguides matched to same density gradient, $A_{10} = A_{20}$). The effect of the power reduction in the outside waveguides is to broaden the principal peak somewhat, analogous to amplitude modulation in the frequency domain, thereby shifting the lower zero closer to $n_z = 1$ and reducing the inaccessible power. Useful powers of 89.6% (95%) between 1.8 and 5.5 and inaccessible powers of 9.5% (4.2%) are achieved for $S_1/S_2 = 1$ (0.42).

It is noted here that the reduction of power in the outside waveguides in order to reduce the inaccessible part of the power was first suggested by Krapchev and Bers (Ref. 7). Their results for a 4-waveguide grill centered at a higher wavenumber are entirely borne out by the present example, except for the fact that their figures should show no power transferred for $0 < |n_z| < 1$ (see discussion after Eq. 26 or 47 above).

From the above, the present WEGA grill is well-adapted to couple almost all the power into the accessible region of the spectrum. The spectrum can, however, not be varied without dramatically increasing the inaccessible power.

b) 12-Waveguide Grill

In order to demonstrate the range of possibilities of spectrum tailoring possible with a multiwave guide grill having a large number of elements, we have chosen as an example a 12-waveguide grill. This grill has about the same total length as the 4-waveguide grill of the previous section, and can thus be used in the next experimental phase of the WEGA program. The frequency considered remains 800 MHz, but the results remain of course applicable if the dimensions are scaled with the frequency. The dimensions are : waveguide width 1.2 cm (b= 0.2), mean separation of waveguides 1.6 cm (p =Δz=0.268), ℓ=12, geometrical wavenumber (Eq. 120 or 103) n_G = 11.7. Total length $L/\lambda o$=0.51. The wavenumber for accessibility remains 1.8. Although the geometrical wavenumber n_G is too high to be of interest in itself, we have chosen this grill to permit flexibility of operation.

The results are given in Table III and Fig. 10-13. Configuration denotes the phasing of the total field used, S_k/S= 1/12 means equal power transmitted by each waveguide. Inaccessible power and the power in the principal peak (between the zeroes on either side) are quoted. The minimum value as a function of ∇n of the global reflection coefficient R, the ratio of reflected to incident power, as well the quality factor Q are given. It is noted that R and Q are not quoted at the same ∇n, since their minima do not coincide, as was already apparent in Fig. 7 for the 4-waveguide grill.

Cases 1-3 in Table III represent the three possibilities, odd, even, and $\pi/2$, of creating a power spectrum with a peak around $n_z = n_G/2$ 5.8 at equal power density transmitted per waveguide. The spectral power densities, normalized to total power transmitted, are plotted in Fig.10. As expected from the discussion of Sec. VI, the even configuration is better, although the improvement of even over odd was more striking at equal total field (Sec. VI) than at equal power density considered here. The inaccessible power is lowest for the even case, although quite low for the other cases also, as is to be expected from the high central n_z used here.

TABLE III : RESULTS OF 12-WAVEGUIDE GRILL

Configuration	Center n_z	S_{k}/S	Inacc. Power	Power Princ. Peak	R_{min}	Q	Fig.
1. Even 0:π:π:0 ...	5.9	1/12	0.3%	85%	16%	2.8	10
2. Odd 0:0:π:π ...	5.5	1/12	4 %	81%	14%	3.4	10
3. Δφ = 90°	5.6	1/12	4.5%	80%	12%	2.7	10(13)
4. Even 0:π:π :0 ...	5.9	.03-.14	3.6%	84%	17%	3.0	11
5. Odd 0:0:π:π ...	5.2	0-.16	0.5%	92%	10%	3.6	11
6. Δφ = 90°	5.6	0-.13	0.5%	88%	10%	3.6	11
7. Odd 0:0:0:π:π:π ...	3.3	1/12	9.7%	83%	19%	3.4	12
8. Odd 0:0:0:π:π:π ...	3.1	.01-.18	3.7%	94%	12%	4.6	12
9. Δφ = 60°	3.6	1/12	9.4%	87%	16%	2.7	12(13)
10. 4-WG Grill	3.1	1/12	9.5%	90%	11%	2.5	9
11. Δφ = 180°	11.7	1/12	1.0%	88%	12%	3.0	13
12. Δφ = 150°	9.7	1/12	2.6%	60%	12%	3.1	13
13. Δφ = 120°	7.7	1/12	3.1%	74%	12%	3.4	13
14. Δφ = 90°(cf.3)	5.6	1/12	4.5%	80%	12%	2.7	13(10)
15. Δφ = 60°(cf.9)	3.6	1/12	9.4%	87%	16%	2.7	13(12)

In cases 4-6 (Fig. 11), the power transmitted by each guide is no longer equal. Instead, we have imposed the condition that each waveguide be matched to the same ∇n (A_{ko}=equal). It is seen from Fig. 11 and Table III that the odd and 90° configurations are improved by this amplitude modulation, i.e. have more power in the principal peak and less inaccessible power. The even configuration is not improved, but for this case A_{ko} is already roughly equal for all the guides at equal power density. It is noted that for the odd and 90° cases, Q increases, which is due to the increase in power density of the central waveguides due to the amplitude modulation. Of these six cases, case 1 (even, equal power density) seems to offer the best compromise between ease of operation (equal power density), concentration of power in the principal peak, and maximization of transferrable power (low Q).

In cases 7-9 of Table III and Fig. 12, several possibilities for creating a peak near $n_G/3$ are presented. For this n_z, the possibility of an even configuration does not exist, since each half period is now made up of an odd number of waveguides (three). For reference, we have included as case 10 in Table III the 4-waveguide grill considered in section VIIIa) above, since it is centered at roughly the same n_z. The equal-amplitude standing-wave case (7) is not quite as satisfactory as case 10 as concerns power in the principal peak, reflection, and Q, although it gives roughly the same inaccessible power. Very strong amplitude modulation (case 8) is neccessary to match the entire grill at the same A_{ko}, with good results as far as the spectrum is concerned, but a strong increase in Q due to the increase in power transferred by the inner waveguides. Here, the best compromise would be to modulate the power densities in order to minimize Q, but this has not yet been carried out. The equal-power travelling-wave case, case 9, is seen to be just as good as the 4-waveguide grill, case 10.

In cases 11-15 various travelling-wave cases are studied. The principal peak of each case is plotted in Fig. 13, except for the 150° case, for which the principal peak for negative n_z is also plotted.

For $\Delta\phi = 180°$, we have a standing wave, and therefore plot the sum of the positive and negative n_z peaks. From the figure, and Table III, it is seen that $\Delta\phi \leq 90°$ and $\Delta\phi = 180°$ give acceptable power fractions in the principal peak ($\Delta\phi = 90°$ can be improved by amplitude modulation, cf. case 6). Phase angles between 90° and 180° are not acceptable, since too much power is taken by the other travelling-wave peak, at negative but high n_z's, and would therefore be lost at the edge. This example confirms the discussion in Sec. VIg.

The 12-waveguide grill presented here is therefore capable of producing standing-wave spectra centered at $n_z \sim 3.3$ and $n_z \sim 5.6$, as well as travelling-wave spectra centered at any n_z between these two values. At any of these wavenumbers, power in the principal peak of more than 85% and inaccessible power of less than 10% may be achieved. Furthermore, neither the global reflection coefficient R nor the quality factor Q, the best ratio of maximum electric field to nominal electric field squared, is significantly changed by going from 4 to 12 waveguides. The grill described here is therefore a well-adapted tool to study, under the same conditions as the WEGA 4-guide grill, coupling to electrons ($n_z = 5.6$) or ions ($n_z = 3.3$), travelling-wave excitation, and dynamic tailoring, and compare the operation of a classical and a multiwaveguide grill.

VIII- CONCLUSIONS :

In the present report, we have developed a formulation, simplified with respect to (8) and extended with respect to (7), of the coupling problem of a multiwaveguide grill, with a view to optimization of the power spectrum. A novel grill configuration, the " even " grill, has been identified and found to be very interesting, because it offers good definition of the principal peak, low inaccessible power, and a good quality factor Q (effective standing-wave ratio) because amplitude modulation is not necessary to improve the definition of the spectrum and it may therefore operate at equal power densities in each waveguide. Of this class of even grills, the three- or five-waveguide grills described in Sec. VII are especially interesting for experiments in which the available port is shorter than a wavelength.

In the framework of our simplified theory, we have shown that the spectral power density produced by the grill depends only on the grill geometry and the total electric fields at the waveguide mouth, as does the power fraction transferred to the plasma by each waveguide. This has permitted us to calculate the quantities which depend on the density gradient at constant power spectrum, which is the real quantity of interest.

By studying the examples described above, as well as a series of other examples not described in detail here, some general considerations have emerged. First, as already remarked in (7) and (8), the 2-waveguide grill, while offering an unacceptable power spectrum, is definitely the best as far as the reflection or the quality factor Q (1.55, Sec.VII) is concerned. This is simply due to the fact that there are only 2 waveguides, which are identical in all the deduced properties by symmetry. However, once one passes to four or more waveguides in order to obtain an acceptable power spectrum, a further increase in the number of waveguides does not lead to a further significant increase in reflections, independent of the number of waveguides, the central n_z, or the production of travelling rather than standing waves.

In fact, this conclusion may be understood qualitatively from Eq. (52) to (56). Once a very good concentration of the electric field in the region $|n_z| > 1$ has been achieved, either by centering at high n_z, using an even configuration, or amplitude modulation in the odd or travelling-wave case, the contribution to the surface admittance Y_k from $|n_z| < 1$ usually becomes negligible for all but the end waveguides of the grill. For the inside waveguides, the largest contribution to Y_k comes from its own field E_k. Hence, for these guides, the phase angle of Y_k is close to -30°, corresponding to a minimum standing-wave ratio $\Gamma_k = 1.7$

It usually turns out when amplitude modulation is used to improve the definition of the power spectrum that the amplitude of the end waveguides must be decreased, and of the inside ones increased. (In fact in some cases, for example case 5 or 8 of Table III, the power transferred by the outside waveguides is almost zero, rendering these guides similar to the " passive " guides in Ref. (14) and giving the same result, i.e. improvement of the power spectrum definition).

Therefore, the quality factor Q_k is never below 1.7, except for the two-waveguide case, but is normally above it by the ratio of power density of inside waveguides to average power density. Since this increase in amplitude is normally not very great, values of Q_k between 2.5 and 4 are typically found independent of the number of waveguides, except in extreme cases where the individual best values of the density gradient lie too far apart.

In order to permit maximum flexibility of the grill, dynamic tailoring, or current production, we also conclude that the geometrical n_G should always be twice as high as the highest n_z which is actually to be used. For the travelling-wave case, it was shown above that phases between 90° and 180° do not give acceptable definition of the power spectrum, leading immediately to this conclusion. However, the statement is also true for the standing-wave case if the " even " configuration is to be used, unless one wishes to use waveguides of unequal width as in the 3 - or 5-waveguide examples presented here. In fact, the best number of waveguides to use per grill is $\ell = 2^k$, permitting the largest variety of odd and even configurations. (The 12-guide grill of the previous section was not ideal in this respect since it did not permit an even configuration at $n_z = 3.3$, whereas the advantage of the even grouping is greater as n_z approaches 1). While the condition $n_G = 2n_{zmax}$ appears necessary from the considerations presented here, technical considerations may change this conclusion, since this conditions demands twice as many waveguides half as wide. For example, it has been pointed out (15) that, if the transmissible power is limited by the multipactor effect (limiting field proportional to waveguide width) that this condition leads to a reduction of the transmissible power by a factor 2, above the quality factor Q.

In conclusion, reduction of the inaccessible power below 10% and optimal definition of the peak of the power spectrum have been shown possible for a multiwaveguide grill, with reflection factors and electric fields similar to those of the classical 4-waveguide grill.

ACKNOWLEDGMENTS

The autor wishes to express his particular thanks to Drs. G.W. PACHER and G.F. TONON for many discussions and suggestions in the course of this work. Fruitful discussions with Drs. J.-G. WEGROWE, M. BRAMBILLA, T.K. NGUYEN and the members of the WEGA Team and the Grenoble laboratory are gratefully acknowledged. Many thanks are also due to Mme ISEPPI for typing the manuscript and R. FRITSCH for drawing the figures.

REFERENCES

1. LALLIA, P., in RF Plasma Heating (Proc. 2nd Top. Conf. Lubbock 1974), paper C3
2. BRAMBILLA, M., Nucl. Fusion 16 (1976), 47.
3. BRAMBILLA, M., in Plasma Heating in Toroidal Devices (Proc. Symp. Varenna, 1976) 84.
4. BRAMBILLA, M., in Controlled Fusion and Plasma Physics (Proc. 7 Europ. Conf. Lausanne, 1975) Vol. 2 (1975) 222.
5. BRAMBILLA, M., Review of the Grill Theory, Report EUR-CEA-FC 890, April 1977.
6. BERNABEI, S., FIDONE, I., in Plasma Heating in Toroidal Devices (Proc. Symp. Varenna 1976) 92.
7. KRAPCHEV, V., BERS, A., Nucl. Fusion 18 (1978), 519
8. BRAMBILLA, M., Nucl. Fusion 19 (1979), 1343
9. GOLANT, V.P., Sov. Phys.- Tech.Phys. 16 (1972), 1980
10. STIX, T.H., The Theory of Plasma Waves, Mc Graw-Hill (1961), Chapter 1
11. PACHER, H.D., BLANC, P., DURVAUX, M., GORMEZANO, C., HESS, W., ICHTCKENKO, G., LALLIA, P., MAGNE, R., NGUYEN, T.K., PACHER, G.W., SOLDNER, F., TONON, G.F., WEGROWE, J.-G., in Plasma Physics and Controlled Nuclear Fusion Research (Proc. 7th Int. Conf. Innsbruck, 1978) Vol. 1, IAEA, Vienna (1979), 97.
12. FISCH, N.J., Phys. Rev. Letters 41 (1978), 873.
13. KARNEY, C.F.F., and FISCH, N.J., Princeton Plasma Physics Laboratory Report PPPL-1506 (Jan. 1979).
14. MOTLEY, R.W., and HOOKE, W.M., Princeton Plasma Physics Laboratory Report PPPL-1606 (Nov. 1979).
15. TONON, G.F., private communication.

FIGURE CAPTIONS

Fig. 1 Periodicity function $\alpha(n_z, n_{zp})$ plotted as a function of n_z/n_{zp} for 1, 2 and 3 complete periods of the exciting field (i.e. at least 2, 4, and 6 waveguides, respectively).

Fig. 2 Configuration function β_c for odd, even, and $\pi/2$ distributions of equal-field-amplitude, equally-spaced waveguides as a function of n_z/n_{zp}. α (Fig.1) and β_c multiplied together give geometrical power density if wall thickness is ignored, and transmitted power density (non-normalized) when divided by $|n_z^2-1|^{2/3}$.

Fig.3 Normalized spectral power density $S(n_z)/\int_{-\infty}^{\infty} S(n_z)dn_z$ (full line) integral, $\int^{n_z} S(n_z)dn_z / \int^{\infty} S(n_z)dn_z$ (dotted line) as a function of n_z for grill G2 ($b_1=b_2=0.785$, $\phi_1=0$, $\phi_2=\pi$) and G3($b_1=b_3=0.449$, $b_2=0.898$, $\phi_1=\phi_3=0$, $\phi_2=\pi$), when field amplitudes at waveguide mouth equal. Zero wall thickness.

Fig.4 Normalized spectral power density $S(n_z)/\int^{\infty} S(n_z)dn_z$ (full line) and integral, $\int^{\infty} S(n_z)dn_z / \int^{\infty} S(n_z)dn_z$ (dotted line) as a function of n_z for grill G4 ($b_1=b_2=b_3=b_4=0.785$, $\phi_1=\phi_3=0$, $\phi_2=\phi_4=\pi$) and G5 ($b_1=b_5=0.449$, $b_2=b_3=b_4=0.898$, $\phi_1=\phi_3=\phi_5=0$, $\phi_2=\phi_4=\pi$) when total field amplitudes at waveguide mouth equal. Zero wall thickness.

Fig.5 Same conditions as Fig.3, except transmitted power density constant.

Fig.6 Same as Fig. 4 except transmitted power density constant.

Fig.7 4-Waveguide Grill WEGA with finite walls. (b=const=0.586, waveguide separation $\Delta z = 0.905$, phases $\phi_1=\phi_3=0$, $\phi_2=\phi_4=\pi$). $n_G= 3.47$, $L/\lambda o=0.58$. Transmitted power S_k/S equal. Plotted are quality factors of inside Q_2, Q_3) and outside (Q_1, Q_4) waveguides, power reflection coefficients of inside $|\rho_{2,3}|^2$ and outside $|\rho_{1,4}|^2$ waveguides and global power reflection coefficient R as a function of ∇n (cm^{-4}) over f_G (frequency in GHz) cubed.

Fig. 8 4-Waveguide Grill WEGA, same geometry and phases as Fig. 7. Results at $\nabla n = 6.7\ (10)^{11} f_G^3\ cm^{-3}$, as a function of ratio of transmitted power in outside (S_1 or S_4) to inside (S_2 or S_3) waveguides. Plotted are quality factors of inside and outside waveguides, transmitted power of inside ($(S_2+S_3)/S$) and outside ($(S_1+S_4)/S$) waveguides, incident power of inside ($(S_{i2}+S_{i3})/S$) and outside ($(S_{i1}+S_{i4})/S$) waveguides, ratio of accessible to total transmitted power S_{acc}/S, and total incident power normalized to transmitted power $\Sigma S_{ik}/S$.
Effective quality factor for accessible power Qmax/(Sacc/S) is also plotted, where Qmax is the larger of Q_1 or Q_2.

Fig. 9 4-Waveguide grill WEGA, same geometry as Fig. 7. Plots of normalized spectral power density $S(n_z) / \int_1^\infty S(n_z)\,dn_z$ (full line) and integral $\int_1^{n_z} S(n_z)\,dn_z / \int_1^\infty S(n_z)\,dn_z$ (dotted line) as a function of n_z. The two cases correspond to equal transmitted power density ($S_1/S_2=1$) and variable transmitted power density ($S_1=S_4:S_2=S_3$ in ratio of 0.42 : 1).
The latter case corresponds to $A_{10}=A_{20}=A_{30}=A_{40}$.

Fig.10 12-Waveguide grill (b= const= 0.2, waveguide separation $\Delta z=0.268$) $n_G= 11.7$, $L/\lambda= 0.51$. Power spectra of odd (dot-dashed line, case 2, Table III), even (dotted line, case 1) and $\pi/2$ (full line, case 3). For standing-wave odd and even cases $(S(n_z)+ S(-n_z)) / \int_{-\infty}^{\infty} S(n_z)\,dn_z$ are plotted, while for travelling-wave odd $\pi/2$ case, $S(n_z) / \int_{-\infty}^{\infty} S(n_z)\,dn_z$ is plotted. Phases are : odd $(0,0,\pi,\pi, \ldots)$, even $(0,\pi,\pi, 0, \ldots)$ and $\pi/2$ $(0 : \pi/2 : \pi : 3\pi/2 \ldots)$.
Equal transmitted power densities.

Fig. 11 Same conditions as Fig. 10, except power densities unequal, adjusted so all A_{ko}'s of each grill are equal. (cases 4-6, Table III).

Fig. 12 Same grill geometry as Fig. 10. Full line is odd configuration at constant transmitted power density, phases $0:0:0:\pi:\pi:\pi \ldots$(case 7, Table III). Dotted line is same configuration, but with unequal power densities, adjusted so all A_{ko}'s are equal (case 8_1). Dotdashed line is travelling-wave configuration at equal transmitted power density, phases 0:60°:120°:180°:240°:300°:... (case 9)

Fig. 13 Same grill geometry as Fig. 10. Relative phases between waveguides as given on the figure. Plotted is $S(n_z)/\int_{-\infty}^{\infty} S(n_z)\,dn_z$ except for 180° case, where we plot $(S(n_z) + S(-n_z))/\int_{-\infty}^{\infty} S(n_z)\,dn_z$ and 150°, where negative peak is also plotted. Only principal peaks are shown. Cases correspond to case 11-15, Table III.

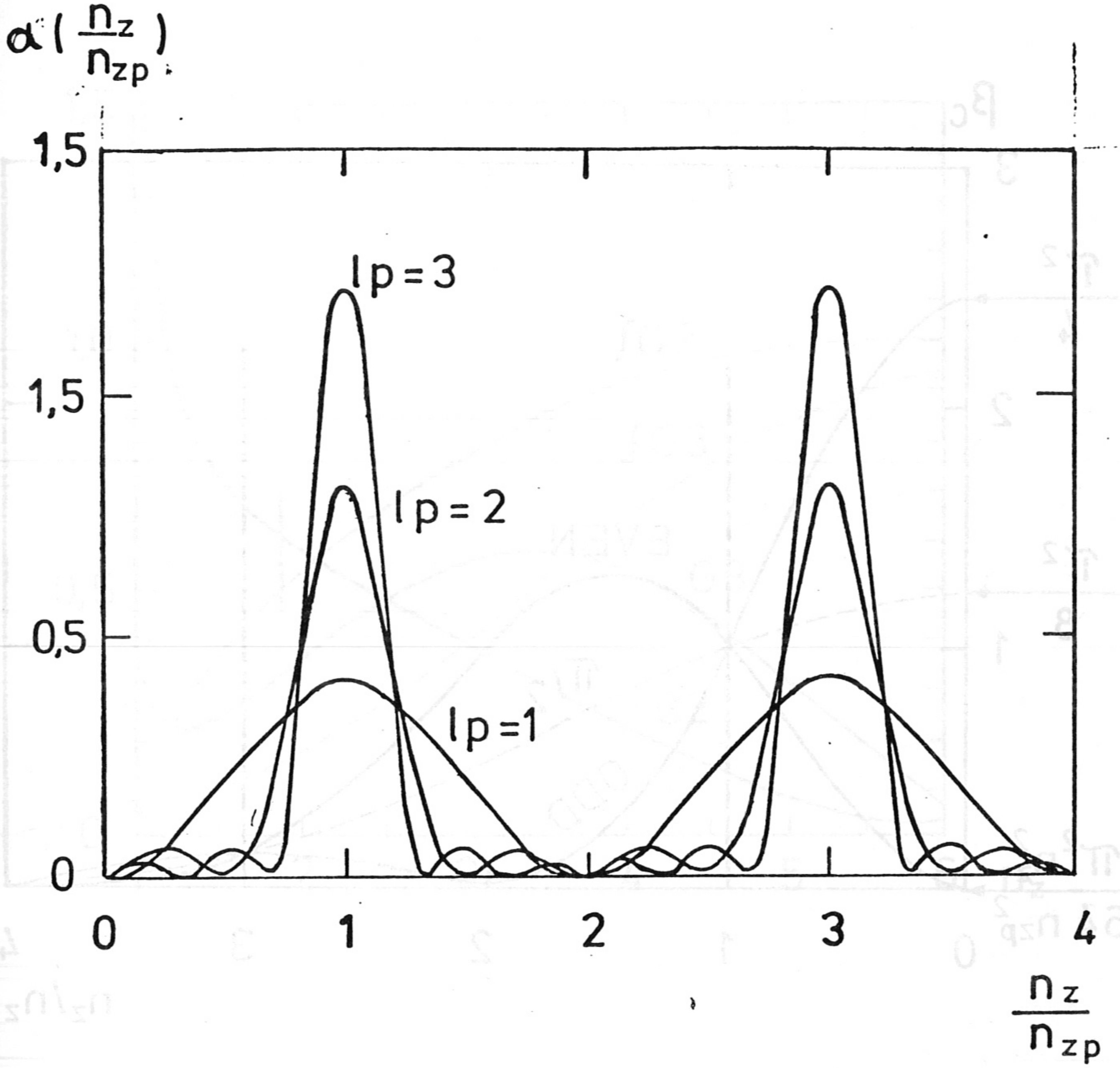

Fig.1

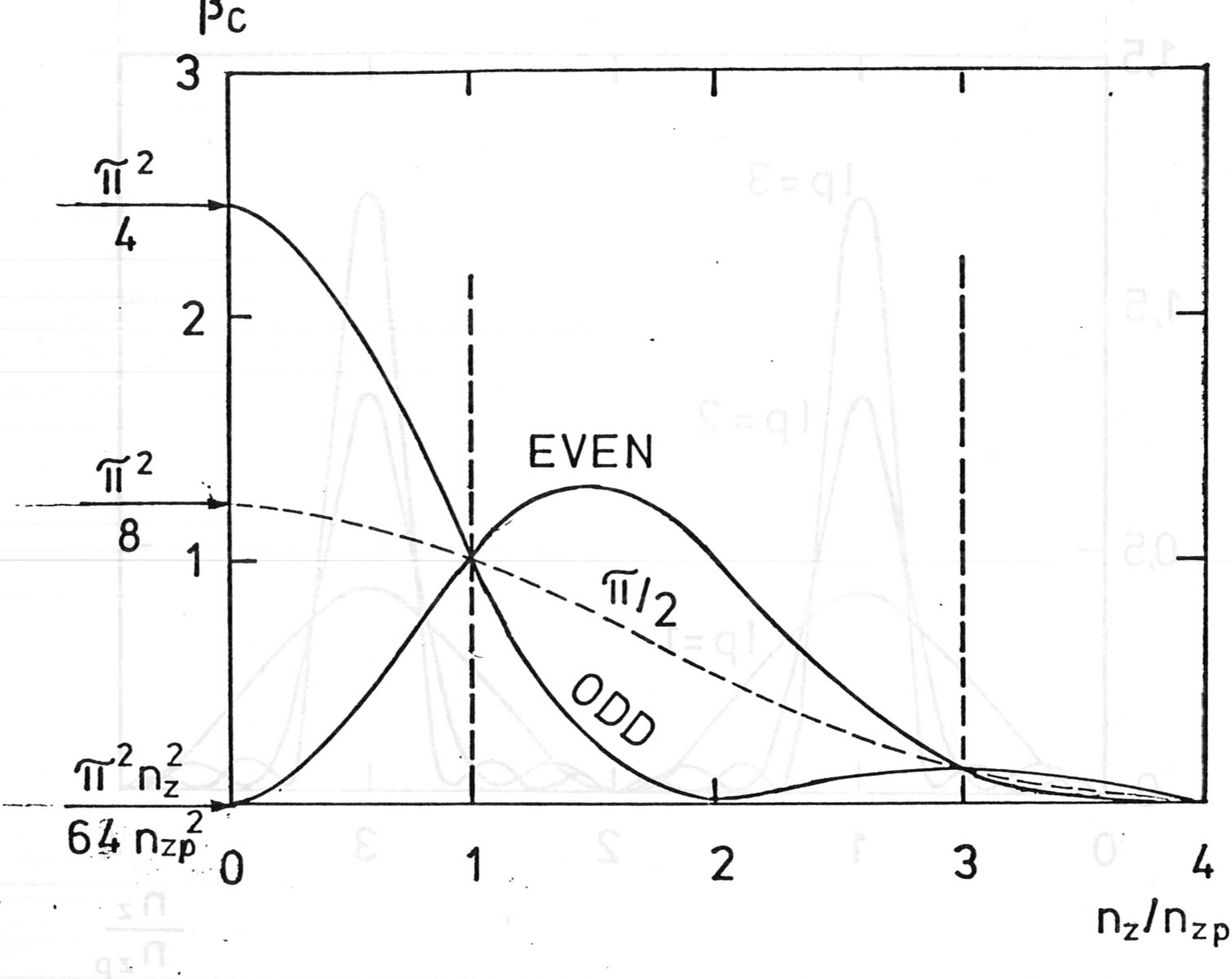

Fig. 2

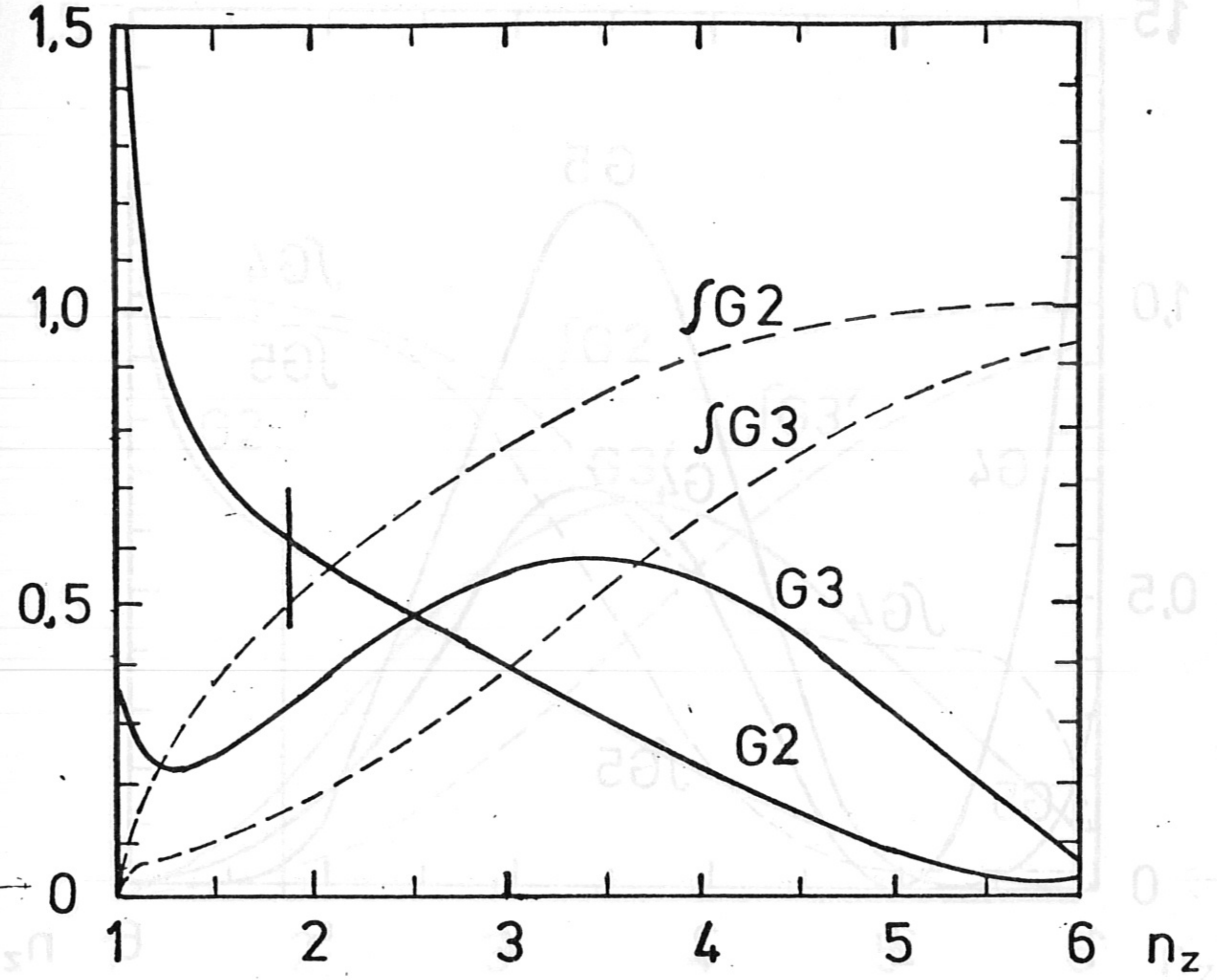

Fig.3

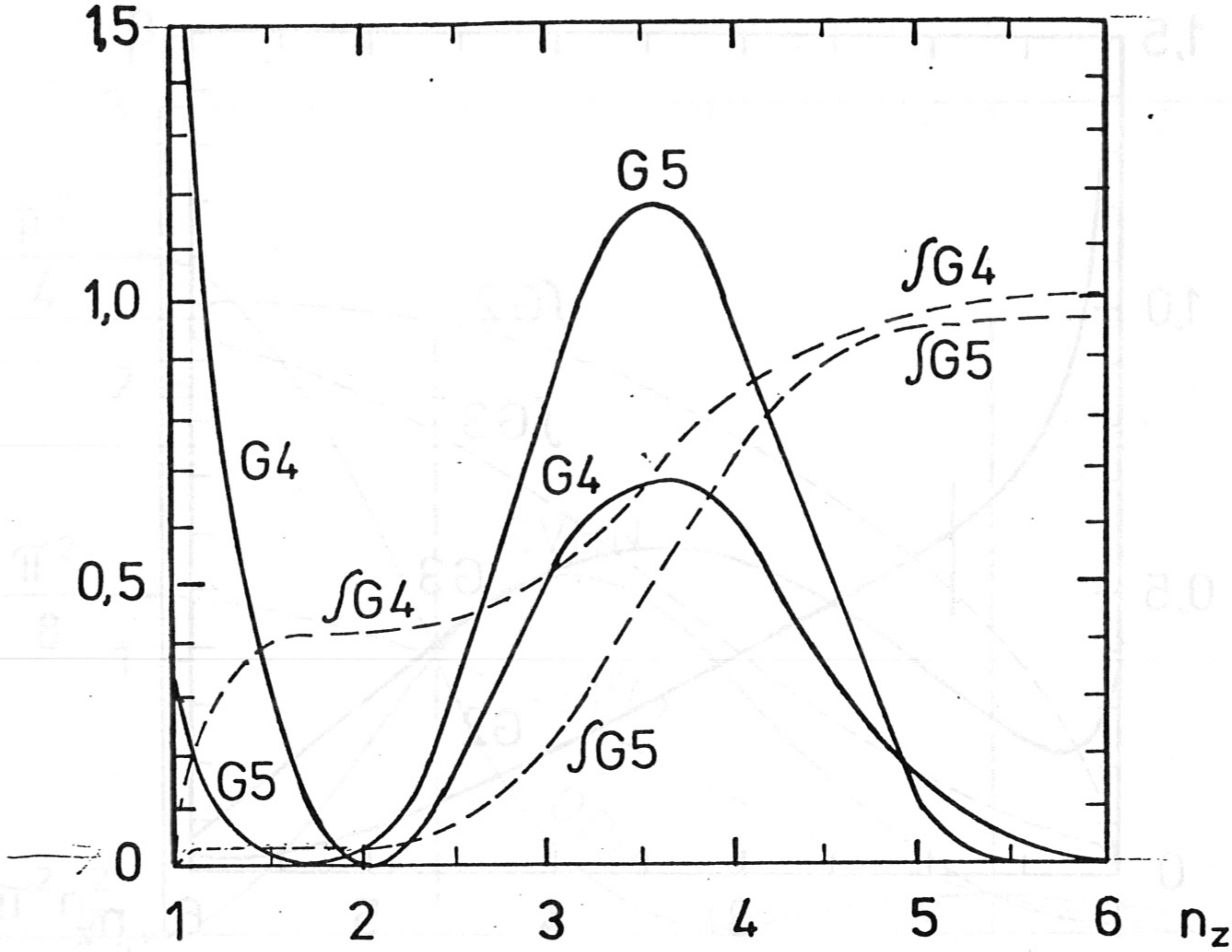

Fig. 4

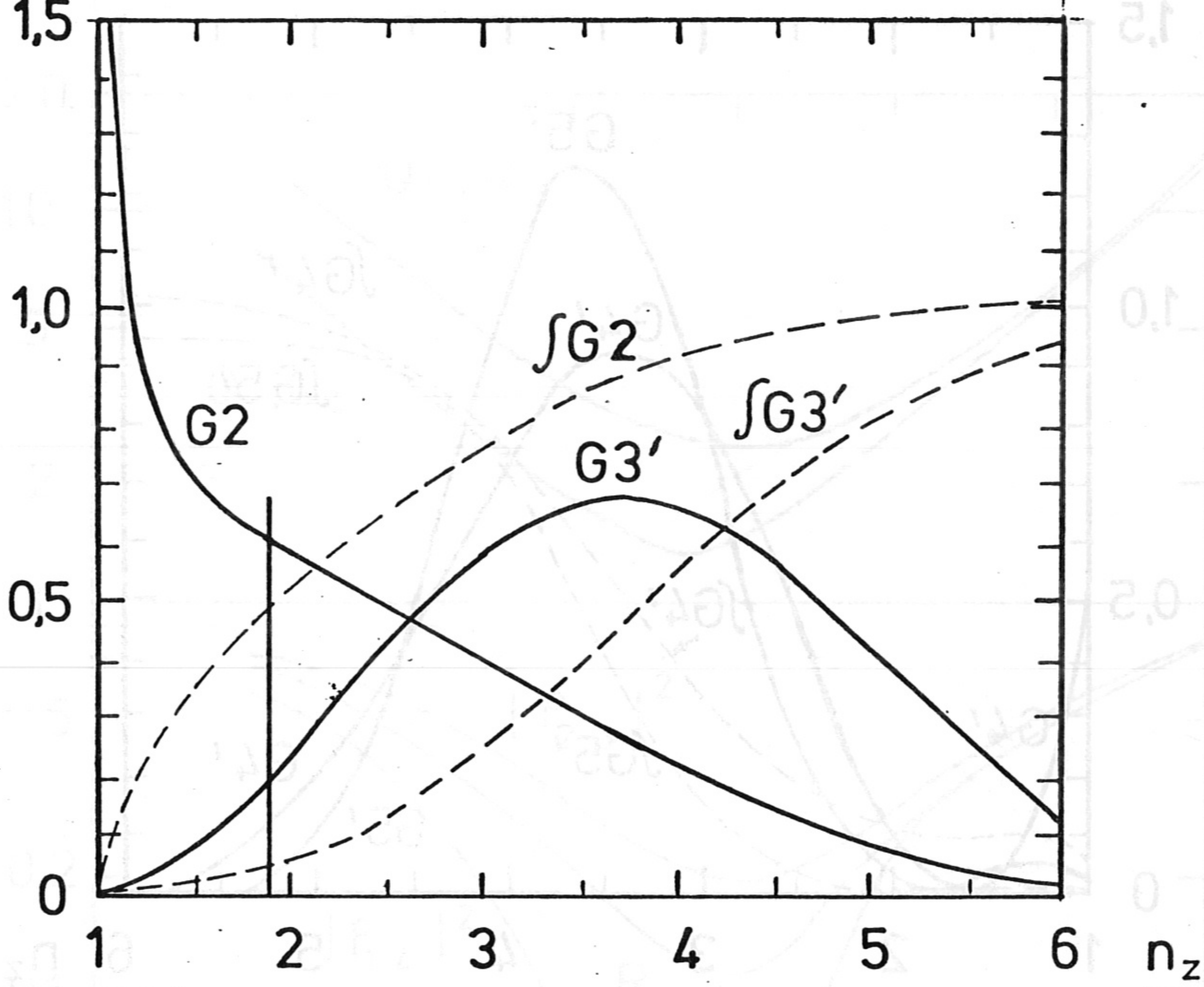

Fig. 5

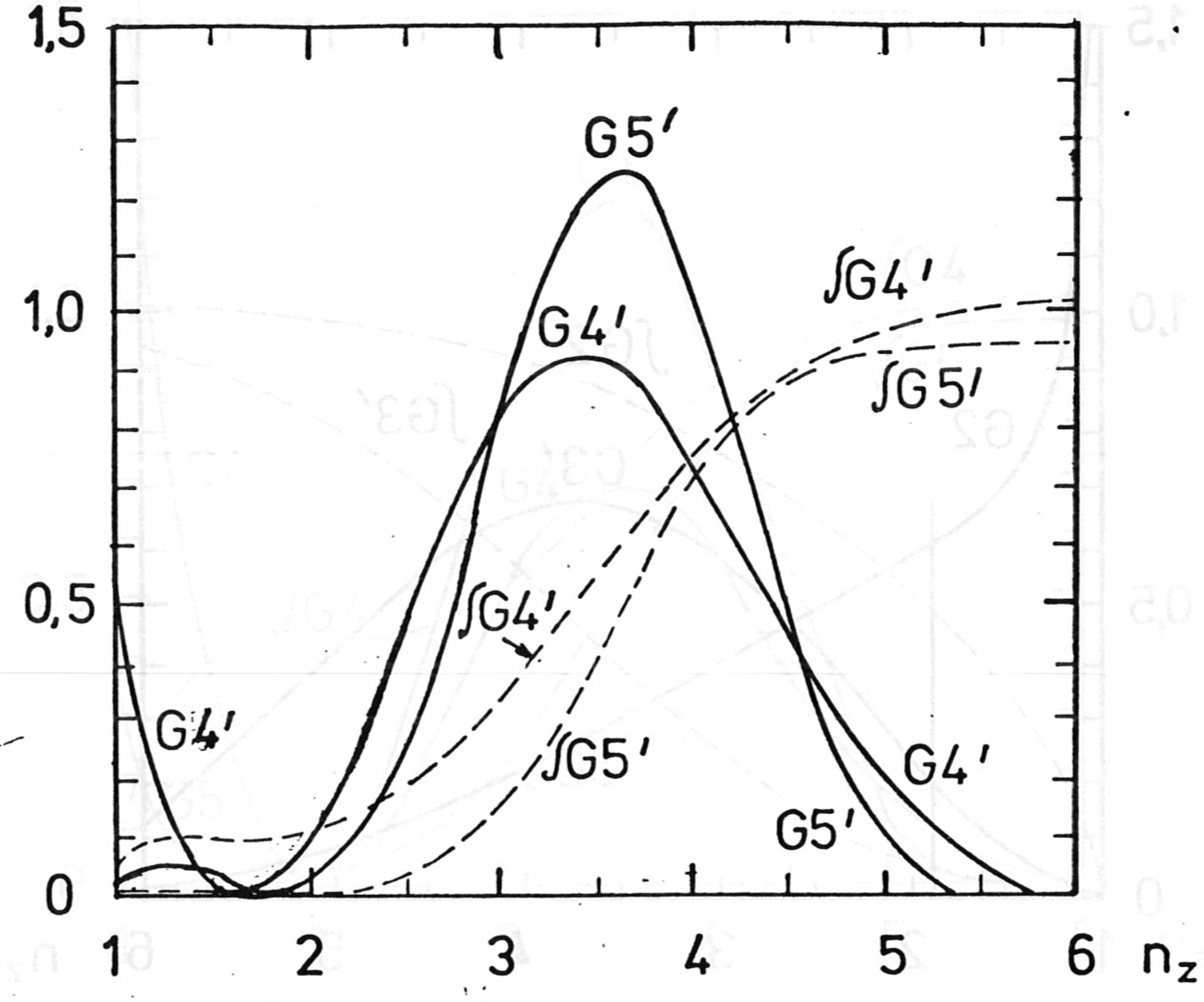

Fig. 6

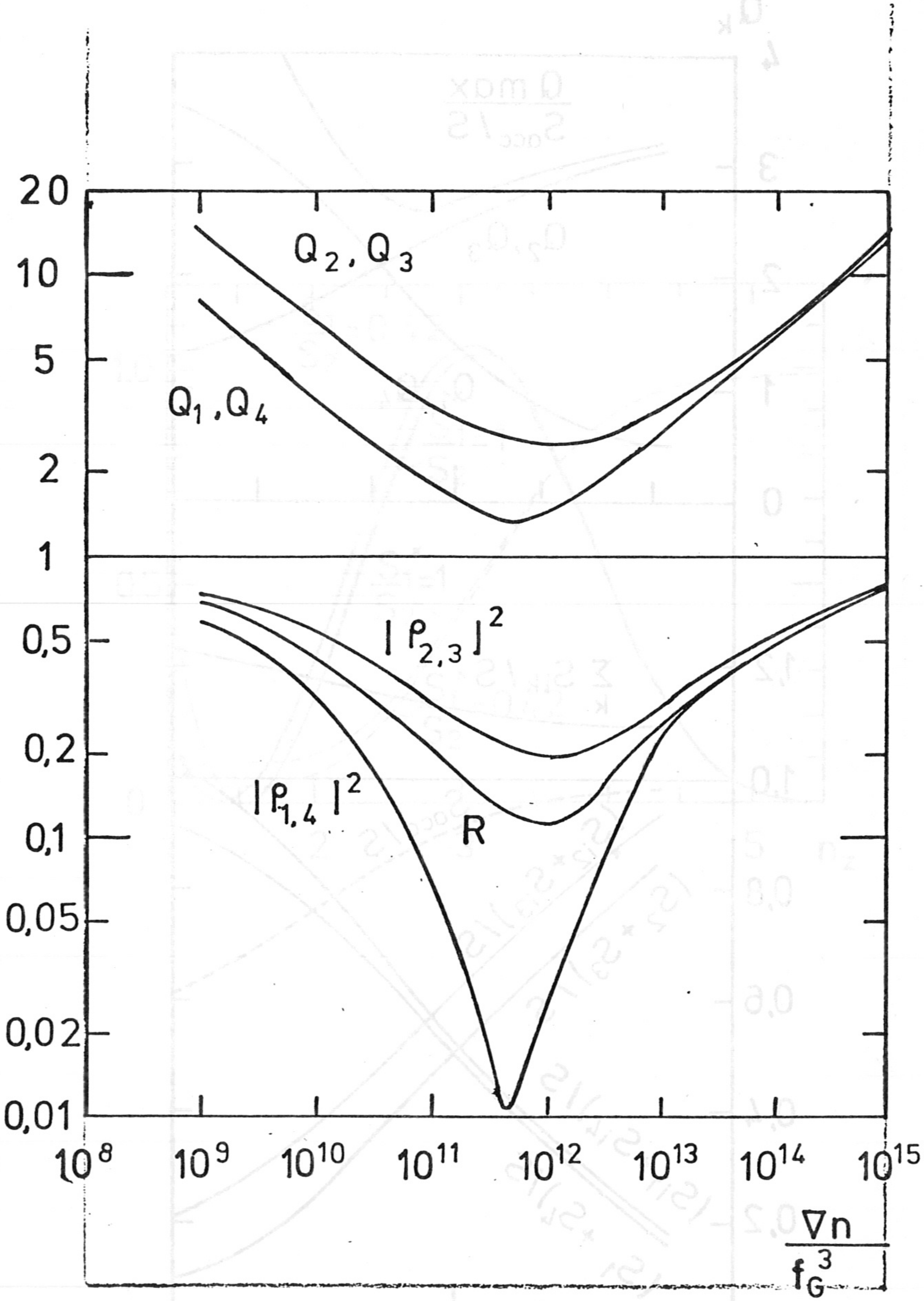
20
10
5
2
1
0,5
0,2
0,1
0,05
0,02
0,01
Q2 , Q3
Q1 , Q4
| ρ2,3 |²
| ρ1,4 |²
R
10^8
10^9
10^10
10^11
10^12
10^13
10^14
10^15
∇n / fG³

Fig. 7

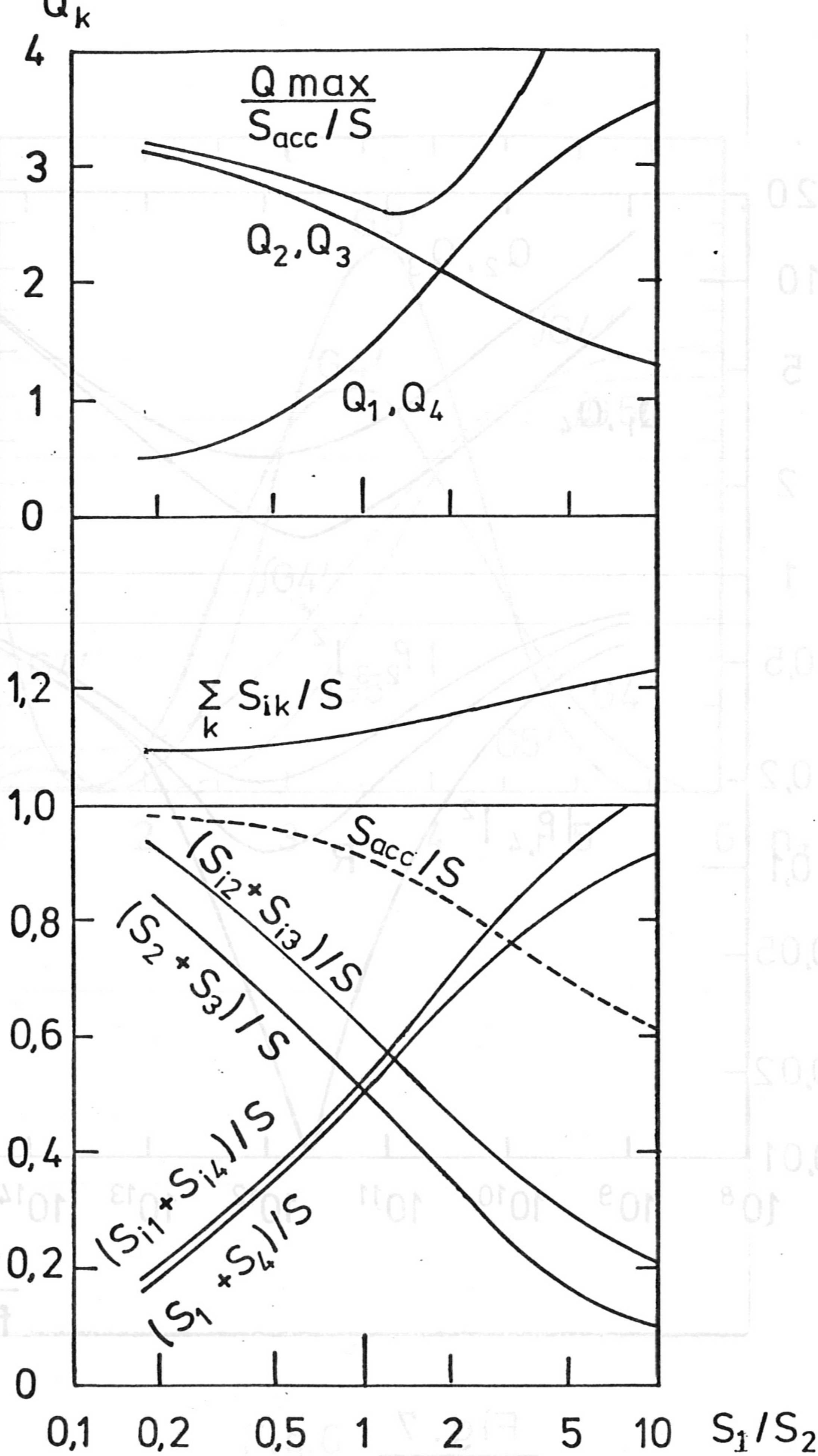

Q k
Q max / S acc / S
Q 2 , Q 3
Q 1 , Q 4
Σ k S ik / S
S acc / S
(S i2 + S i3)/S
(S 2 + S 3)/S
(S i1 + S i4)/S
(S 1 + S 4)/S
4
3
2
1
0
1,2
1,0
0,8
0,6
0,4
0,2
0
0,1
0,2
0,5
1
2
5
10
S 1 /S 2

Fig. 8

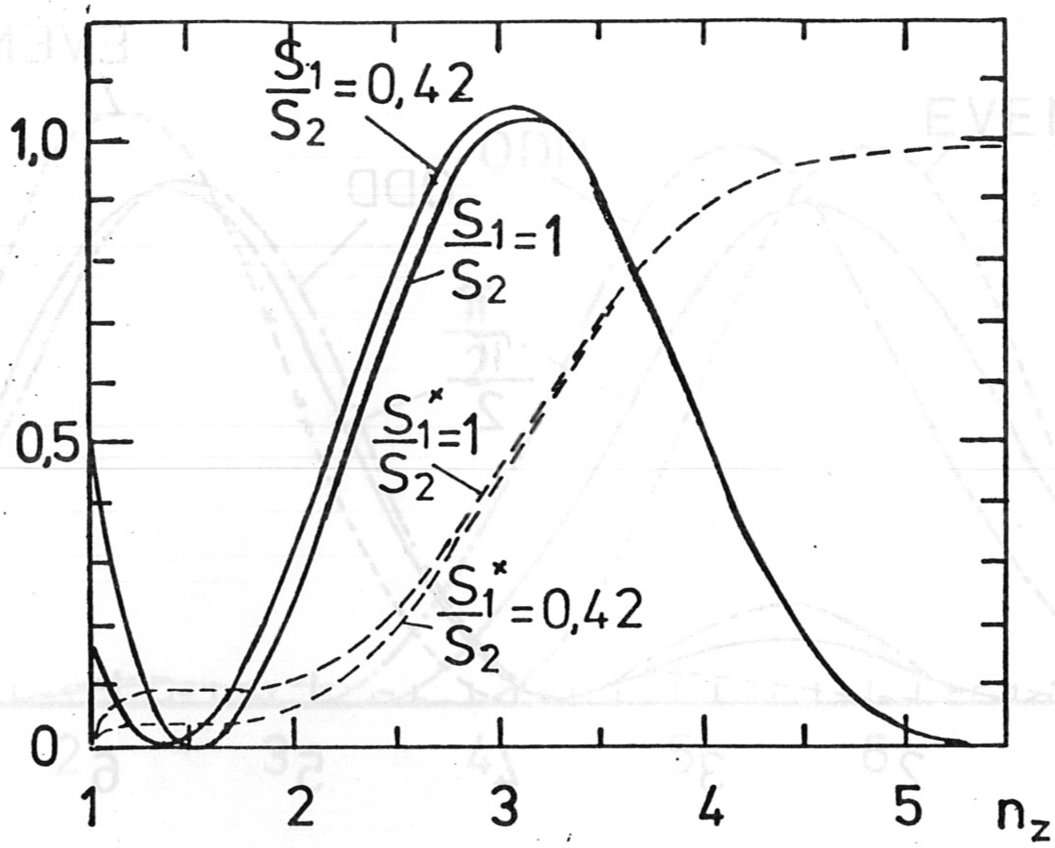
$\frac{S_1}{S_2}=0,42$
$\frac{S_1}{S_2}=1$
$\frac{S_1^*}{S_2}=1$
$\frac{S_1^*}{S_2}=0,42$
1,0
0,5
0
1
2
3
4
5
n_z

Fig. 9

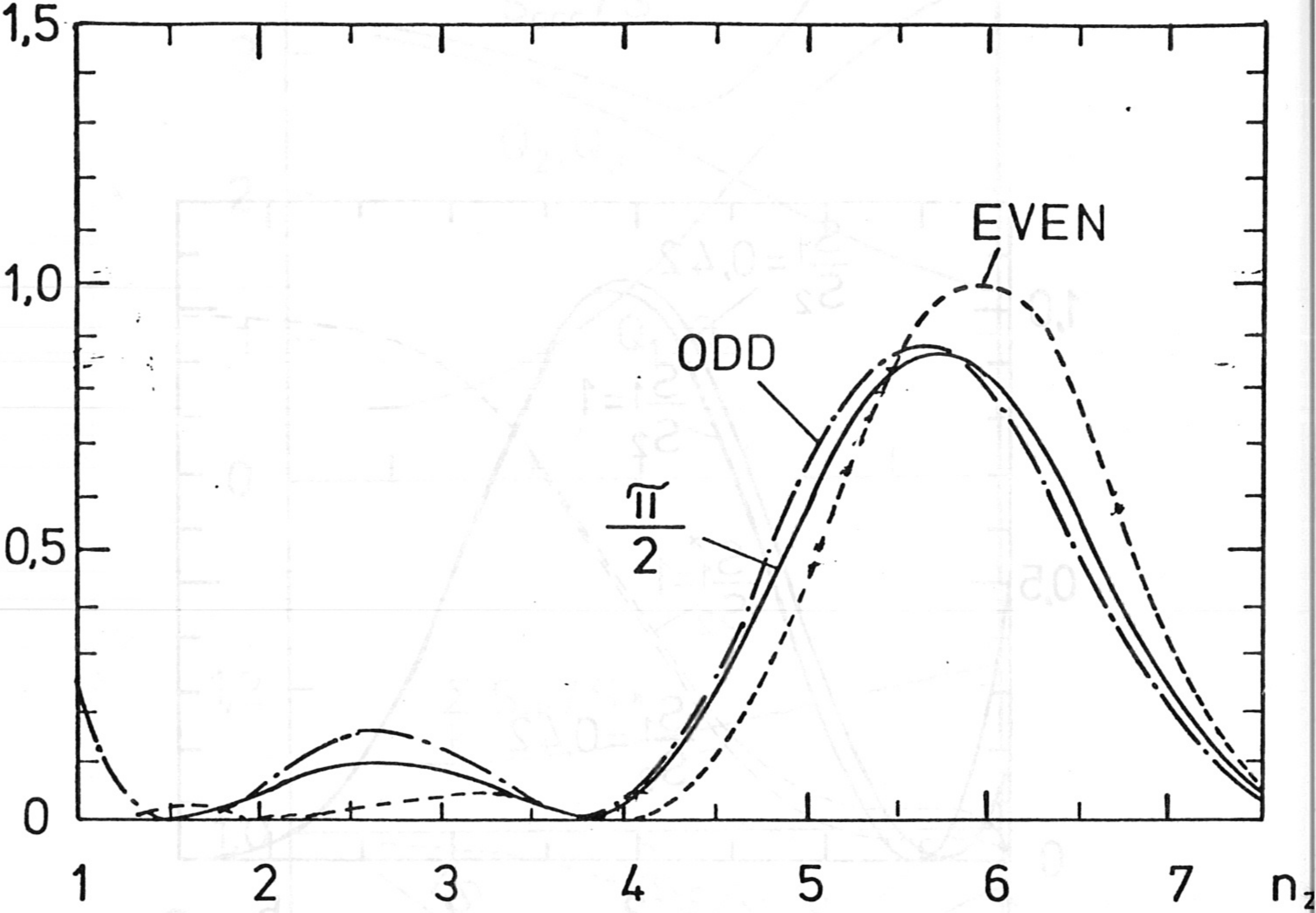

Fig. 10

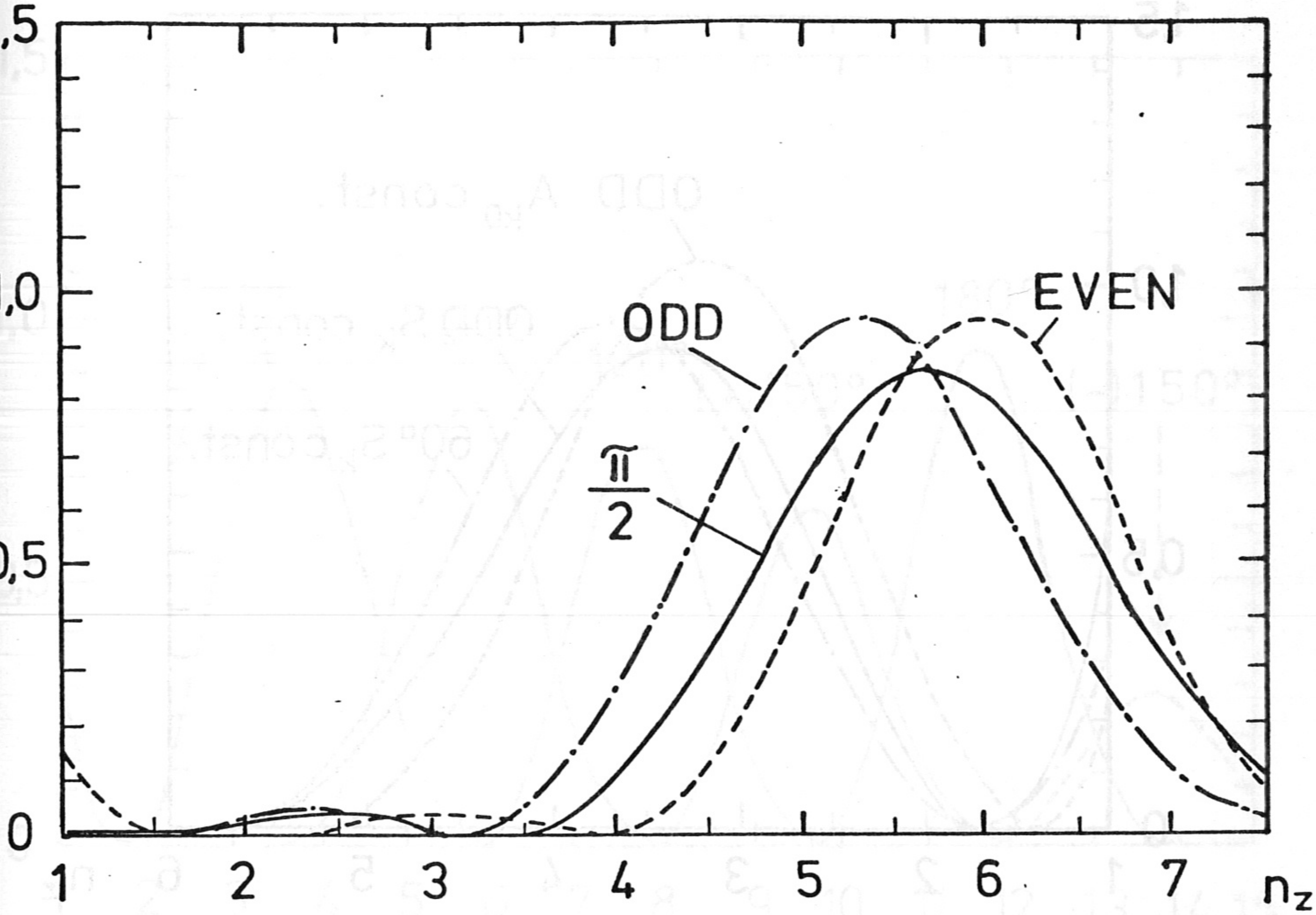

Fig.11

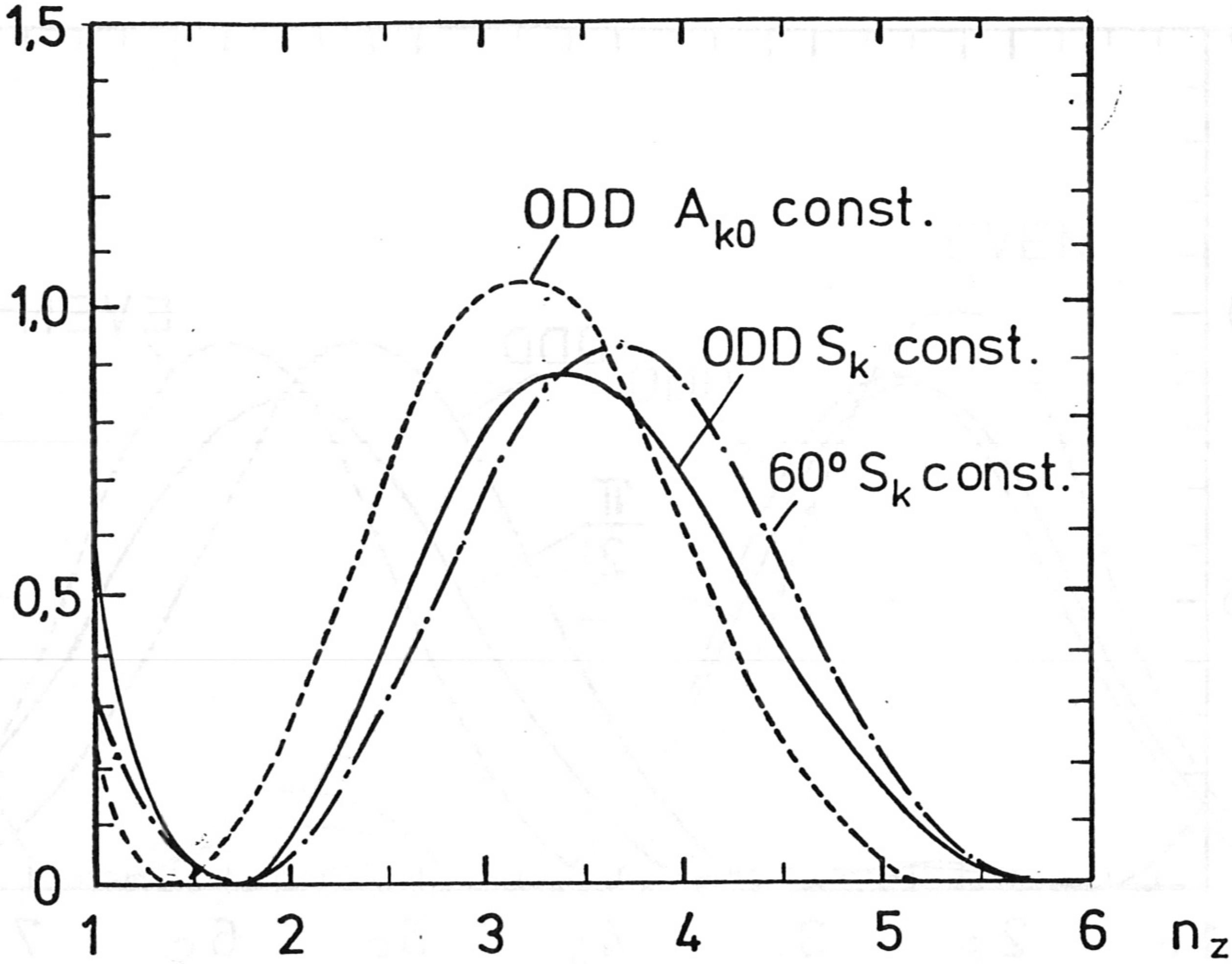

Fig.12

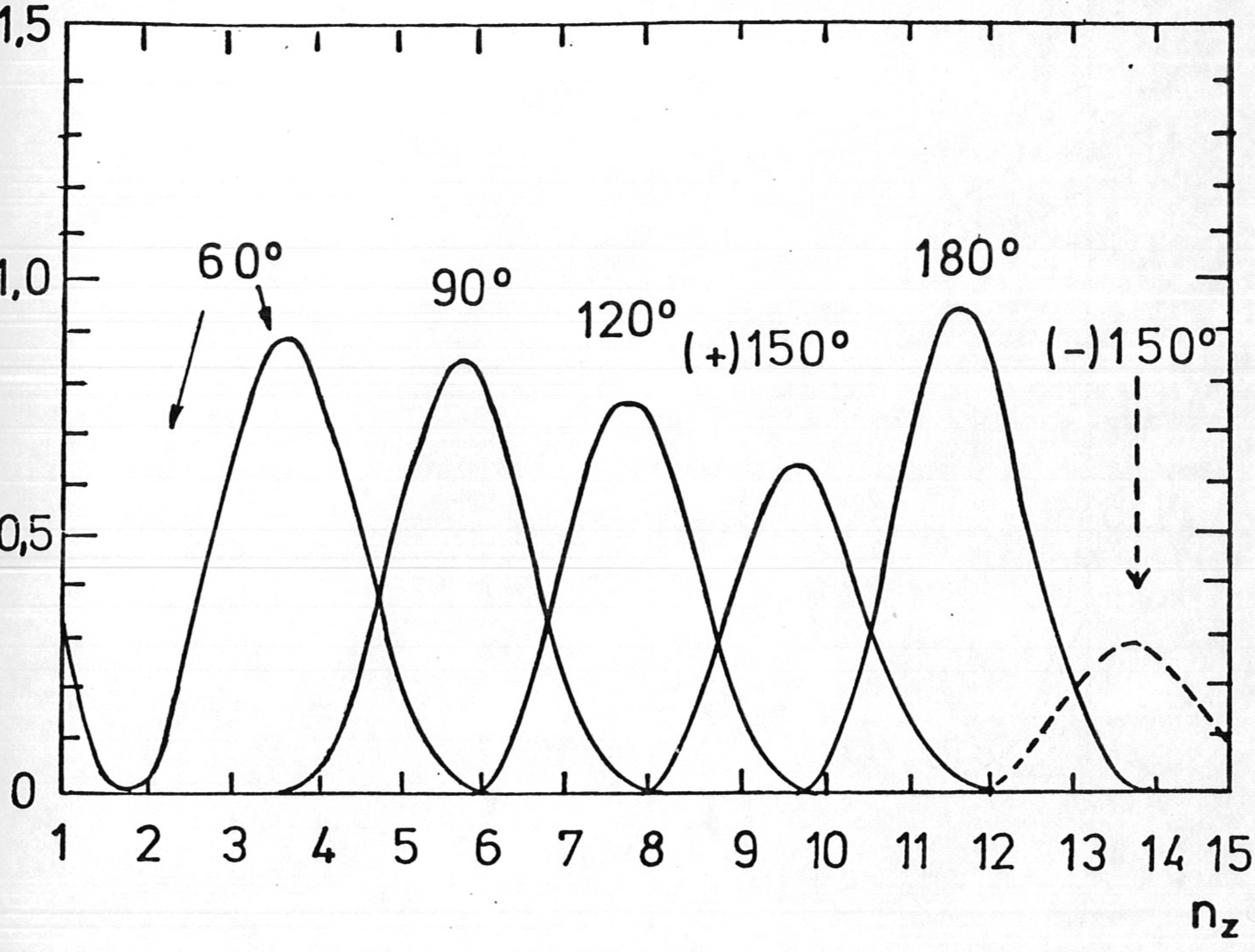

Fig. 13